JAERI-M
84-239

ANNUAL REPORT OF THE OSAKA LABORATOYY FOR RADIATION CHEMISTRY JAPAN ATOMIC ENERGY RESEARCH INSTITUTE

(No. 17)

April 1, 1983－March 31, 1984

January 1985

Osaka Laboratory for Radiation Chemistry

日 本 原 子 力 研 究 所
Japan Atomic Energy Research Institute

JAERI-M レポートは、日本原子力研究所が不定期に公刊している研究報告書です。

入手の問合わせは、日本原子力研究所技術情報部情報資料課（〒319-11 茨城県那珂郡東海村）あてお申し越しください。なお、このほかに財団法人原子力弘済会資料センター（〒319-11 茨城県那珂郡東海村日本原子力研究所内）で複写による実費頒布をおこなっております。

JAERI-M reports are issued irregularly.

Inquiries about availability of the reports should be addressed to Information Division, Department of Technical Information, Japan Atomic Energy Research Institute, Tokai-mura, Naka-gun, Ibaraki-ken 319-11, Japan.

編集兼発行　日本原子力研究所
印　　刷　日立高速印刷株式会社

JAERI-M 84-239

ANNUAL REPORT OF THE OSAKA LABORATORY FOR RADIATION CHEMISTRY JAPAN ATOMIC ENERGY RESEARCH INSTITUTE (No. 17)

April 1, 1983 - March 31, 1984

Osaka Laboratory for Radiation Chemistry
Takasaki Radiation Chemistry Research Establishment, JAERI

(Received December 17, 1984)

This report describes research activities of Osaka Laboratory for Radiation Chemistry, JAERI during one year period from April 1, 1983 through March 31, 1984. The latest report, for 1983, is JAERI-M 83-199.

Detailed descriptions of the activities are presented in the following subjects: studies on surface phenomena under electron and ion irradiations; polymerization under the irradiation of electron beams; modification of polymers, degradation, cross-linking, and grafting.

Previous reports in this series are:

Annual Report,	JARRP,	Vol. 1	1958/1959*
Annual Report,	JARRP,	Vol. 2	1960
Annual Report,	JARRP,	Vol. 3	1961
Annual Report,	JARRP,	Vol. 4	1962
Annual Report,	JARRP,	Vol. 5	1963
Annual Report,	JARRP,	Vol. 6	1964
Annual Report,	JARRP,	Vol. 7	1965
Annual Report,	JARRP,	Vol. 8	1966
Annual Report,	No. 1,	JAERI 5018	1967
Annual Report,	No. 2,	JAERI 5022	1968
Annual Report,	No. 3,	JAERI 5026	1969
Annual Report,	No. 4,	JAERI 5027	1970
Annual Report,	No. 5,	JAERI 5028	1971
Annual Report,	No. 6,	JAERI 5029	1972
Annual Report,	No. 7,	JAERI 5030	1973
Annual Report,	No. 8,	JAERI-M 6260	1974
Annual Report,	No. 9,	JAERI-M 6702	1975
Annual Report,	No.10,	JAERI-M 7355	1976
Annual Report,	No.11,	JAERI-M 7949	1977
Annual Report,	No.12,	JAERI-M 8569	1978
Annual Report,	No.13,	JAERI-M 9214	1979
Annual Report,	No.14,	JAERI-M 9856	1980
Annual Report,	No.15,	JAERI-M 82-192	1981
Annual Report,	No.16,	JAERI-M 83-199	1982

* Year of the activities

Keywords: Electron Beam Irradiation, γ-Irradiation, Radiation-Induced Reaction, Polymerization, Grafting, Polymer Modification, Polystyrene, Radiation Chemistry, Auger Spectrum, Gallium Arsenide, Alumina, Silica Gel, Adsorption, Desorption

昭和58年度日本原子力研究所大阪支所年報（No.17）

（１９８３年４月１日～１９８４年３月31日）

日本原子力研究所・高崎研究所・大阪支所

（１９８４年12月17日受理）

本報告は、大阪支所において昭和５８年度に行なわれた研究活動を述べたものである。主な研究題目は、電子あるいはイオン照射下の界面現象に関する基礎研究、電子線照射による重合反応の研究、ポリマーの改質および上記の研究と関連して重合反応、高分子分解、架橋ならびにグラフト重合に関する基礎的研究などである。

日本放射線高分子研究協会年報	Vol. 1		1958／1959
日本放射線高分子研究協会年報	Vol. 2		1960
日本放射線高分子研究協会年報	Vol. 3		1961
日本放射線高分子研究協会年報	Vol. 4		1962
日本放射線高分子研究協会年報	Vol. 5		1963
日本放射線高分子研究協会年報	Vol. 6		1964
日本放射線高分子研究協会年報	Vol. 7		1965
日本放射線高分子研究協会年報	Vol. 8		1966
日本原子力研究所大阪研における放射線化学の基礎研究No.1	JAERI 5018		1967
日本原子力研究所大阪研における放射線化学の基礎研究No.2	JAERI 5022		1968
日本原子力研究所大阪研における放射線化学の基礎研究No.3	JAERI 5026		1969
日本原子力研究所大阪研における放射線化学の基礎研究No.4	JAERI 5027		1970
日本原子力研究所大阪研における放射線化学の基礎研究No.5	JAERI 5028		1971
日本原子力研究所大阪研における放射線化学の基礎研究No.6	JAERI 5029		1972
日本原子力研究所大阪研における放射線化学の基礎研究No.7	JAERI 5030		1973
Annual Report, Osaka Lab., JAERI, No. 8	JAERI-M 6260		1974
Annual Report, Osaka Lab., JAERI, No. 9	JAERI-M 6702		1975
Annual Report, Osaka Lab., JAERI, No.10	JAERI-M 7355		1976
Annual Report, Osaka Lab., JAERI, No.11	JAERI-M 7949		1977
Annual Report, Osaka Lab., JAERI, No.12	JAERI-M 8569		1978
Annual Report, Osaka Lab., JAERI, No.13	JAERI-M 9214		1979
Annual Report, Osaka Lab., JAERI, No.14	JAERI-M 9856		1980
Annual Report, Osaka Lab., JAERI, No.15	JAERI-M 82-192		1981
Annual Report, Osaka Lab.,, JAERI, No.16	JAERI-M 83-199		1982

CONTENTS

I. INTRODUCTION

Osaka Laboratory was founded in 1958 as a laboratory of the Japanese Association for Radiation Research on Polymers (JARRP), which was organized and sponsored by some fifty companies interested in radiation chemistry of polymers. The JARRP was merged with Japan Atomic Energy Research Institute (JAERI) on June 1, 1967, and the laboratory has been operated as Osaka Laboratory for Radiation Chemistry, Takasaki Radiation Chemistry Establishment, JAERI. The research activities of Osaka Laboratory have been oriented towards the fundamental reseach on applied radiation chemistry.

The results of the research activities of the Laboratory were published from 1958 until 1966 in the Annual Reports of JARRP which consisted essentially of original papers. During the period between 1967 and 1973, the publication was published as a JAERI Report which also consisted mainly of original papers. From 1974, the Annual Report has been published as a JAERI-M Report which contains no original papers, but presents outlines of the current research activities in some detail. Readers who wish to have more information are advised to contact with individuals whose names appear under subjects.

The present annual report covers the research activities of the Laboratory between April 1, 1983 and March 31, 1984.

In addition to the continued research program on "radiation research on polymers", a new research program was initiated this year in place of "the effect of radiation on the reaction of carbon monoxide, methane, and hydrogen" which had been carried out during the past nine years accumulating systematic data on the yields of the reaction products required for C_1 chemistry by the end of fiscal 1982. The new research program includes radiation effects on surface phenomena with emphasis on adsorption and desorption of gases on the surface of insulating material, which is related to the development of basic information that will lead to improved understanding of the phenomena occurred on the first wall surface of future nuclear

fusion reactors.

Studies have been carried out in an attempt to clarify the relation between desorption of adsorbed water from the surface of insulating material and change of the surface structure as well as the formation of secondary ion upon electron and argon ion irradiation. This year, silica gel, alumina, and magnesia were selected as insulating materials. From the changes of Auger spectrum of silica gel and alumina during simultaneous bombardment of electron and argon ion, it was concluded that the irradiation resulted in the reduction of the surface due to bond scission at the surface. The amount of secondary ions containing hydrogen atom was found to closely related to the amount of water adsorbed on the surface, and the kinetic analysis of the secondary ion current led to the desorption cross section of $1.4 \cdot 10^{-17}$ cm^2.

A preliminary study to prepare chemically active or inactive surface by electron beam recoil doping on solid surfaces has been carried out on silicon or silica gel surface and iron as injecting element. No definite conclusion has yet obtained from the change in Auger spectrum during argon ion sputtering.

The effect of electron irradiation on short circuit current of a GaAs solar cell was studied to accumulate information that will help understanding trap cite production by irradiation at solid-solid interface between p- and n-regions.

In the study to assign the thermoluminescence centers of polymeric materials for understanding coloration mechanism of film dosimeters, it was found that the thermoluminescence peaks appeared at three different temperature regions in low density polyethylene were affected by the purification procedures of material and by atmosphere in which the film samples were irradiated.

In the radiation research on polymers, studies have been carried out on the preparation of thin polymer films on inorganic substrate directly from monomers and of graft layers on polymer substrate having different morphology and structure.

A flow type of reaction vessel to polymerize monomers in

vapor phase was constructed and preliminary studies using the reaction vessel were carried out on styrene, acetylene and phenylacetylene to prepare thin polymer films. The morphological features and properties of the films were investigated.

Grafting of acrylic acid onto stretched polyethylene fiber pre-irradiated in air has been carried out, and the degree of grafting was measured as a function of time under different reaction conditions such as grafting temperature, and concentration of Mohr's salt to inhibit homopolymerization. Grafted carbon was also prepared and its electric resistance and mutual solubility to polyethylene were also evaluated.

A change in the laboratory administration took place on April 1. Dr. M. Hatada was appointed director in place of Dr. I. Kuriyama who was appointed to director for Division of Research and Development at Takasaki Research Establishment.

Dr. Motoyoshi Hatada, Director
Osaka Laboratory for Radiation Chemistry
Japan Atomic Energy Research Institute

II. RECENT RESEARCH ACTIVITIES

1. Electron and Ar^+ Ion Impact Effects on SiO_2, Al_2O_3 and MgO

A preliminary study of the electron- and Ar^+ ion impact effects on silica gel surface[1] indicated that silica gel undergoes surface reduction under electron impact and that the formation of the hydrogenated secondary ions, $SiOH^+$ and Si_2OH^+, by simultaneous impact with Ar^+ and electrons is closely related to the presence of water adsorbed on the surface. The time dependence of the ion currents of the secondary ions provided us with the Ar^+ ion impact-induced desorption cross-section of water from silica gel. The study has been extended to two other popular insulators, alumina (Al_2O_3) and MgO with a principal purpose to see if these insulators behave similarly to silica gel under electron and Ar^+ ion impact.

The experimental apparatus has been described previously.[1] Silica gel, Al_2O_3 and MgO in powder form were obtained from commercial sources, and pressed to pellets of 0.1 ∿ 0.3 mm in thickness. The water contents as determined by a thermogravimetric analysis (Shinku Riko TGD-3000) were 18.2 wt·% for silica gel, 7.6% for alumina and 7.5% for MgO. The specimen was mounted on a sample holder equipped with an ohmic heater in the analysis system. The temperature was measured with a chromel-alumel thermocouple in contact with the surface of the specimen.

Auger spectrum of Al_2O_3 consists of Al(Ox) around 55 eV, O_{KLL} around 508 eV and Al_{KLL} around 1400 eV where Al(Ox) denotes the signal arising from the interatomic $Al(L_{2,3})O(L_{2,3})O(L_{2,3})$ transition. C_{KLL} signal due to contamination was also observed around 270 eV. Depending on the analysis point of the sample, the peak energies of these signals shift equally in the range of ·5 eV and the intensity of C_{KLL} varies by a factor of 10, showing inhomogeneity of the surface in charge accumulation and surface concentration of atoms.

Continuous electron impact on Al_2O_3 resulted in the decrease of the intensities of Al(Ox) and O_{KLL} in the Auger spectrum. At the same time, a new signal due to metallic Al, Al(M) appeared around 65 eV and grew in intensity with time. The rate of these spectral changes varied from point to point of the analysis with different intensity of C_{KLL}, and no spectral change was observed even by electron impact for 1 hr at the point where the intensity of C_{KLL} exceeds ca. 30% of that of O_{KLL}. Accordingly, the following measurements were carried out on the sample which had been sputtered by simultaneous impact with Ar^+ ions and electrons for ca. 30 min which reduced the intensity of C_{KLL} to below 1% of that of O_{KLL}.

Figure 1 shows the variation of peak-to-peak intensity for Al(Ox), Al(M) and O_{KLL} during and after impact with electrons of 1.5 keV on Al_2O_3. The intensities of these three peaks tend

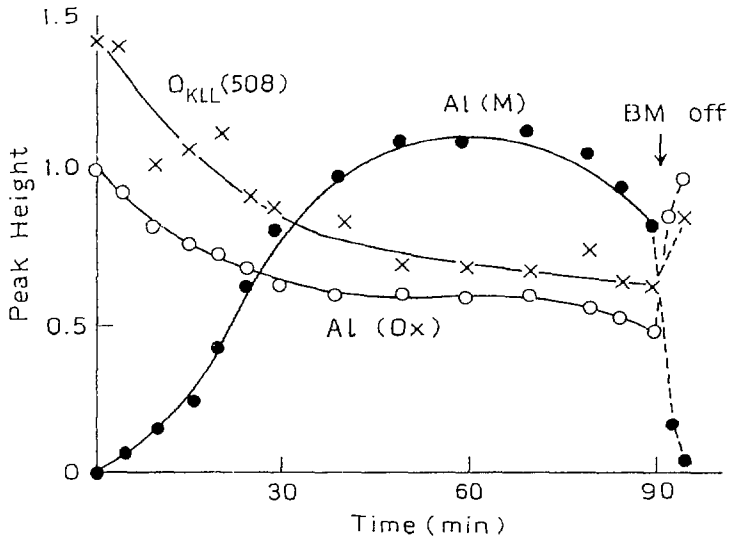

Fig. 1 Variation of Auger peak heights for Al(Ox), Al(M) and O_{KLL} during impact of 1.5 keV electrons on alumina. Peak heights are normalized to the initial peak height for Al(Ox).

to level off ca. 60 min following electron impact, the ratio of the intensities of Al(M) to Al(Ox) being ca. 2 in the final stage. Further impact results in the decrease of the intensities of all the three signals owing to charging up. As can be seen from Fig. 1, when the electron impact was interrupted, Al(M) disappeared in several minutes with concomitant increase of the intensities of Al(Ox) and O_{KLL}.

These results are analogous to those found for silica gel[1], indicating that alumina undergoes surface reduction by electron impact as well as silica gel. In order to estimate the content of metallic Al produced on the alumina surface from the Auger signal intensity, it is necessary to obtain the Auger sensitivity ratio of Al(M) to Al(Ox). For this purpose, Auger spectrum of a fully oxidized Al was recorded before and after sputtering by simultaneous impact with Ar^+ and electrons. The spectral change observed in this experiment was similar to that for Al_2O_3, except that the spectrum in the final stage was exclusively due to metallic Al.[2] The ratio of intensity of Al(M) observed after sputtering and that of Al(Ox) before sputtering was ca. 6 : 1. Using this ratio, the content of metallic Al on the Al_2O_3 surface in the final stage of electron impact was estimated to be ca. 30%.

The effect of the energy of incident electrons on the formation of metallic Al from Al_2O_3 was studied in the energy range from 0.5 and 3 keV. The results are shown in Fig. 2 which indicates that the efficiency increases abruptly when electron energy exceeds 1.5 keV, and decreases above the energy of 2 keV. This finding parallels with the fact that the ionization cross section of K shell electrons in O atom peaks at 2 keV of incident electrons.[3] Therefore, it is suggested that surface reduction of alumina by electron impact is initiated by formation of a core hole in O atom, followed by an intra-atomic Auger process and desorption of O^+ via the "Coulomb explosion".[4,5] In fact O^+ as well as H^+ desorbed from Al_2O_3 were detected in the mass spectrum during impact of electrons above 0.5 keV but the low yield of O^+ (10^{-12} A) prevented us from obtaining the dependence on the energy of incident

electrons.

In contrast to silica gel and Al_2O_3, neither electron impact nor simultaneous impact with Ar^+ ions and electrons on MgO induced any change at all in the Auger electron spectrum. According to the criteria[6] for the stability of ionically bonded solids in an ionizing environment, MgO is labile to electron impact. We have no explanation for the discrepancy at present.

As reported already[1], the Ar^+ ion impact-induced desorption cross section of water from silica gel was obtained from the time dependence of the ion currents of secondary ions

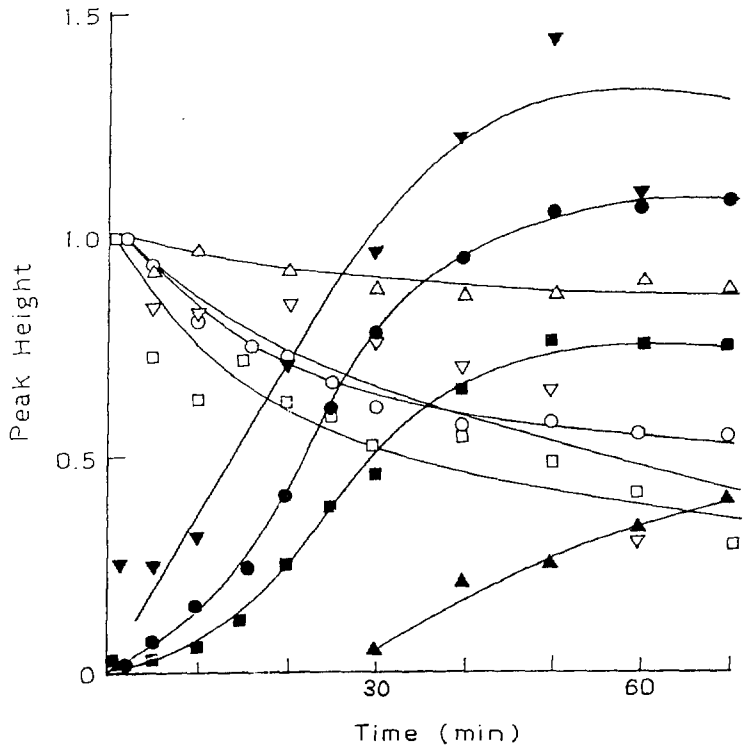

Fig. 2 Variation of Auger peak heights for Al(Ox) (open symbols) and Al(M) (closed symbols) during impact on alumina with electrons of 1 keV (Δ), 1.5 keV (○), 2 keV (▽) and 3 keV (□).

produced by the simultaneous impact with Ar^+ and electrons on silica gel. The analysis was based on eq. 1.

$$(i^+ - i_\infty^+)/(i_0^+ - i_\infty^+) = \exp\{-(JQ/\varepsilon)t\} \qquad (1)$$

where i^+ and i_∞^+ are the initial and final values, respectively, of $SiOH^+$ and Si_2OH^+ ion current, J and ε are the current density and charge of Ar^+ ions, and Q is the desorption cross section of water.

In an attempt to obtain supporting evidence for the validity of the analysis, an experiment was carried out on residual gas analysis during simultaneous impact with Ar^+ and electrons on silica gel, while the currents of four dominant ions, H_2^+, H_2O^+, CO^+ and CO_2^+, being monitored with the aid of a multi-channel ion selector. The currents of all the four ions showed a rapid increase immediately after initiation of the impact, followed by gradual decrease with time, as shown in Fig. 3. Plots of the H_2O^+ ion currents observed in this experiment according to eq. 1 are shown in Fig. 4. The fact that the plot lies close to those for $SiOH^+$ ion currents,

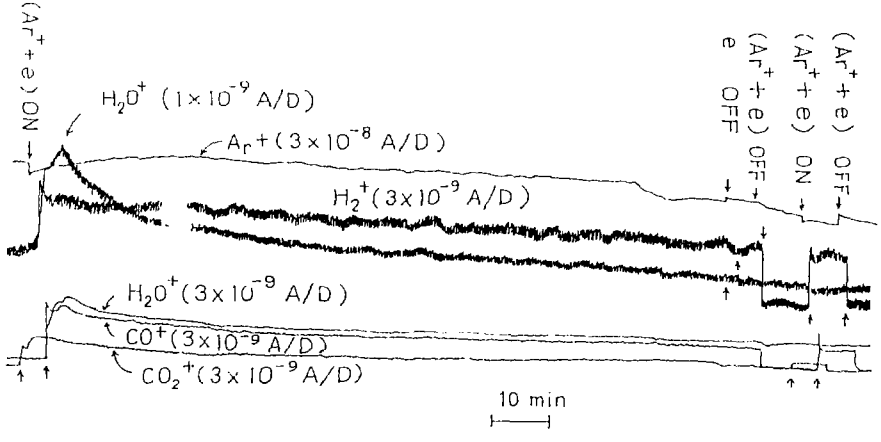

Fig. 3 Recording traces of m/e = 2, 18, 40 and 44 ion currents observed by residual gas analysis during and after simultaneous impact of Ar^+ and electrons on silica gel.

giving the same value of Q as previously obtained desorption cross section of water, confirms the validity of our method to derive the cross section from the time dependence of $SiOH^+$ ion current.

In accordance with the results for silica gel[1], simultaneous impact with Ar^+ and electrons on Al_2O_3 and MgO produced secondary ions in good yields. Ar^+ ion imapct on the insulators produced the same secondary ions as well, but their yields were two orders of magnitude lower than those by the simultaneous impact.

Secondary ions observed from MgO were Mg^+, MgO^+ and $MgOH^+$. The currents of MgO^+ and $MgOH^+$ ions were

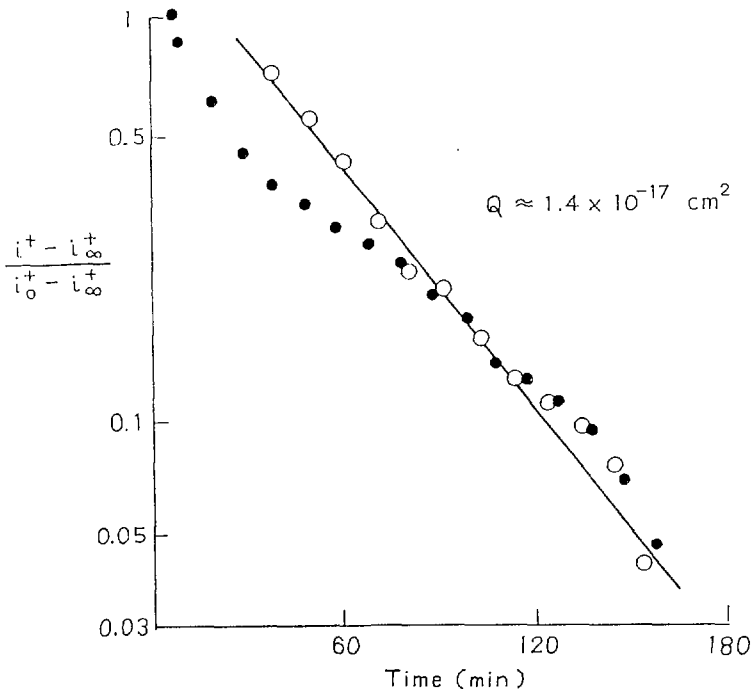

Fig. 4 Plots of H_2O^+ ion currents (closed circles) observed by residual gas analysis during the simultaneous impact, according to eq. 1. Open circles denote the plots for the ion currents of $SiOH^+$.

not determined in the present study because of interference of their mass spectra by an impurity ion K^+ and the source ion Ar^+.

Figure 5 shows the time dependence of ion currents of secondary ions, Al^+, AlO^+, $AlOH^+$ and Al_2O^+ produced from Al_2O_3 during the simultaneous impact of 4 keV Ar^+ and 1.5 keV

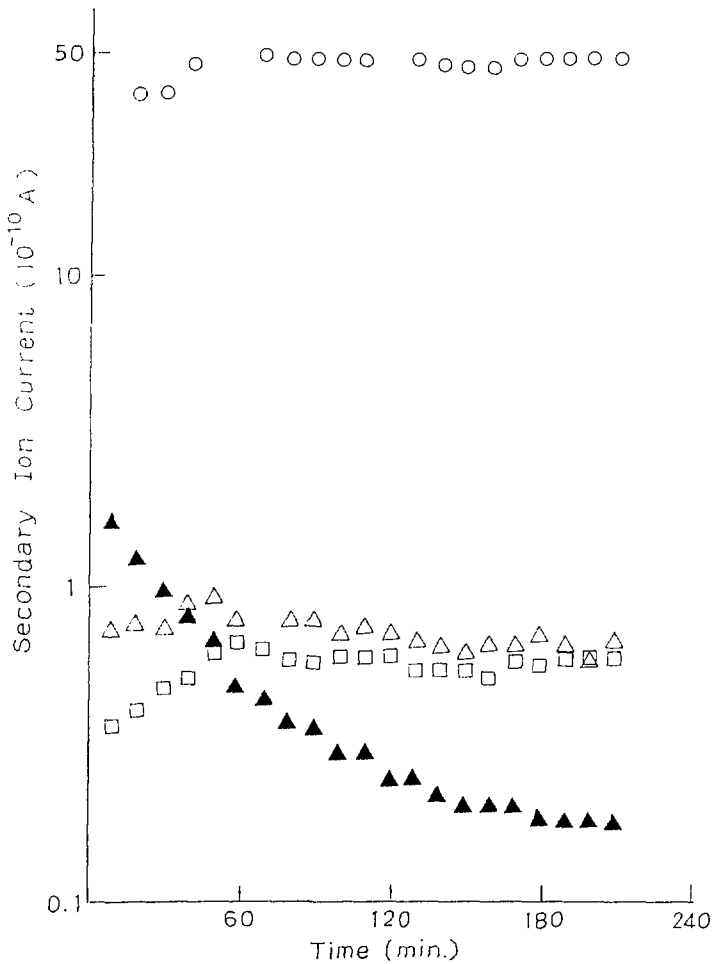

Fig. 5 Time dependence of the ion currents of Al^+ (○), AlO^+ (△), $AlOH^+$ (▲) and Al_2O^+ (□) during simultaneous impact of Ar^+ ions and electrons on alumina.

Table 1 Ar^+ Ion Impact-Induced Desorption Cross Section (Q) of Water Adsorbed on Silica Gel and Alumina

	Energy of Ar^+ (keV)	Q (10^{-17} cm^2)
Silica gel	2	2.3
	4	1.4
Alumina	2	2.2
	4	1.6

electrons. It can be seen that $AlOH^+$ shows a decrease in ion current with time in contrast to the other three secondary ions. Plots of the ion currents of $AlOH^+$ according to eq. 1 gave a straight line, the slope of which provided an estimate of Q to be 2.2×10^{-17} cm^2. Table 1 summarizes the desorption cross sections of water adsorbed on silica gel and alumina with two different energies of Ar^+ ions.

(S. Nagai and Y. Shimizu)

1) S. Nagai and Y. Shimizu, JAERI-M 83-199, 40 (1983); in Secondary Ion Mass Spectrometry, SIMS IV, Springer-Verlag (1984), p. 463.
2) D. T. Quinto and W. D. Robertson, Surf. Sci., 27, 645 (1971).
3) C. J. Powell, Rev. Mod. Phys., 48, 33 (1976).
4) M. L. Knotek and P. J. Feibelman, Phys. Rev. Lett., 40, 964 (1978).
5) P. J. Feibelman and M. L. Knotek, Phys. Rev., 18, 653 (1978).
6) M. L Knotek and P. J. Feibelman, Surf. Sci., 90, 78 (1979).

2. Structure and Decomposition of the Carbonaceous Solid Produced on the Surface of Molecular Sieve-5A by Irradiation of Methane

In the last annual report[1], it was reported that the carbonaceous solid produced by irradiation of methane in the presence of molecular sieve (MS) 5A is highly abundant in carbon atoms, C/H ≈ 7.0 ∿ 9.8. The present study was carried out in an attempt to examine the structure and the behavior of decomposition of the carbonaceous solids deposited over MS 5A and silica gel during irradiation of methane. For this purpose, Auger spectra and X-ray diffraction patterns of the carbonaceous solid on MS 5A or silica gel were measured, and the products by electron impact under an H_2 atmosphere and by H_2^+ ion bombardment on the solids were analyzed by a quadrupole mass filter. For comparison, similar experiments were carried out on silicon carbide (Furuuchi Chemicals Co.) and graphite (Nakarai Chemicals Co.).

Measurement of Auger spectrum and product analysis were carried out with an AES/SIMS equipment described previously.[2] Samples of carbonaceous solids deposited on MS 5A and silica gel were prepared by irradiation of methane with electron beams (0.6 MeV, 2 mA) in the presence of MS 5A and silica gel for 183 min at 300°C.[3] The amount of the carbonaceous solid deposited on MS 5A was estimated to be ca. 5 wt% of MS 5A from the amount of low-molecular-weight hydrocarbons produced when the carbonaceous solid was reirradiated with electron beams for 430 min at 350°C in the flowing H_2. The amount of the solid on silica gel was not determined but supposed to be much lower than that on MS 5A. These samples, silicon carbide and graphite in powder form were pressed to pellets in ∿ 0.5 mm thickness. The specimen was mounted on a sample holder in the stainless steel vacuum chamber which could be resistively heated, and the temperature was monitored with a chromel-alumel thermocouple in contact with the surface of the specimen. The specimen was heated in an ultrahigh vacuum system for 60 min at 300°C before measurements. Auger spectrum of specimen was recorded with primary

electron beam energy of 1.5 keV using 2 V_{pp} modulation. Residual gas analysis was carried out during electron impact (3 keV) under an H_2 atmosphere (1×10^{-6} Torr) and during H_2^+ ion bombardment (3 keV) using a quadrupole mass spectrometer. X-ray diffraction patterns of the samples in powder form were obtained with an X-ray diffraction apparatus (Geiger Flex, D-S type, Rigaku Denki) using nickel filtered copper K_α radiation of 30 kV, 20 mA.

As shown in Fig. 1, Auger spectrum of the carbonaceous solid on MS 5A shows carbon Auger peaks near 275 eV, together with Auger peaks assigned to aluminum (55 eV), silicon (84 eV), calcium (310 eV) and oxygen (510 eV) that are the constituents of MS 5A. Figure 2 shows the carbon Auger spectra of the carbonaceous solids on MS 5A (a) and on silica gel (b), silicon carbide (c) and graphite (d). It is well known that the line-shapes of the small peaks on the low energy side of the main

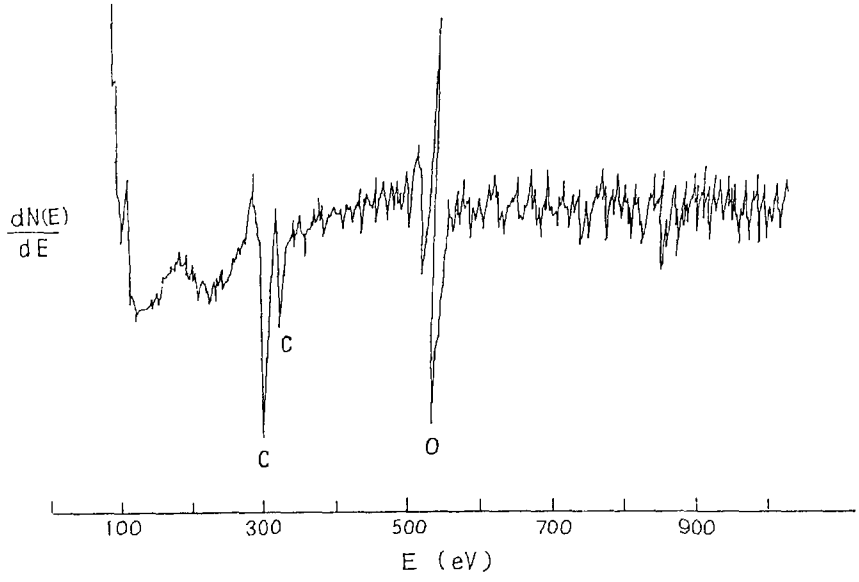

Fig. 1 Auger spectrum of carbonaceous solid deposited on MS 5A: primary electron beam energy, 1.5 keV; modulation, 2 V_{pp}.

peak in the carbon Auger peaks (240 ~ 275 eV) due to the carbon KLL Auger transition are sensitive to the form in which carbon is present at a surface.[4,5] As can be seen from Fig. 2, the lineshapes of the carbon Auger spectra of the carbonaceous solids on MS 5A and silica gel (a and b) resemble that of graphite (d) rather than silicon carbide (c), indicating that the carbonaceous solids on MS 5A and silica gel have a graphite-like carbon structure.

Figure 3 shows ion currents of hydrocarbon ions observed during electron impact under an H_2 atmosphere of the carbon-

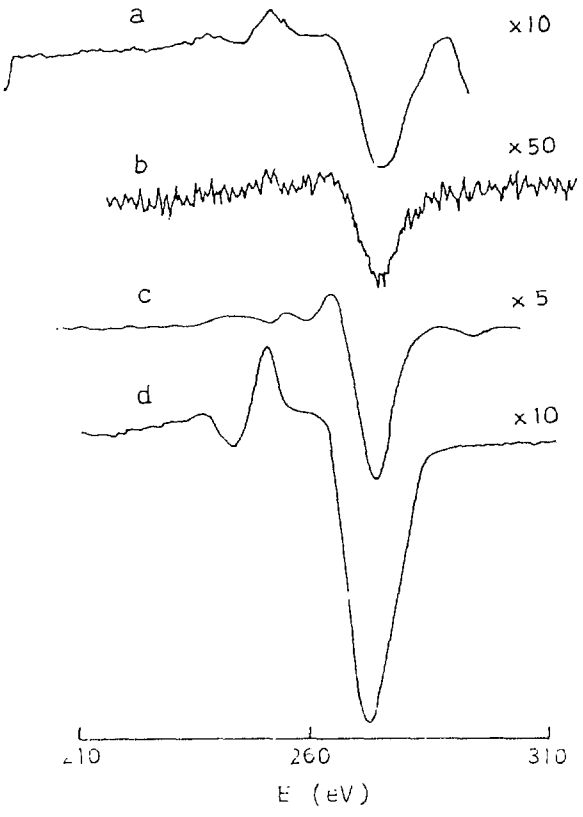

Fig. 2 Carbon Auger spectra of carbonaceous solid on MS 5A (a), on silica gel (b), SiC (c) and graphite (d).

aceous solid on MS 5A, as a function of impact time and temperature. The concentrations of hydrocarbon products increased with increasing impact temperature, and raising the impact temperature to 300°C resulted in an increase in all the concentrations of hydrocarbons produced. In particular, the concentrations of methane produced at 300°C was ca. 3 times that at 55°C. In addition, ethylene and propylene were found to be produced at temperatures above 200°C. These results qualitatively agree with those obtained previously by the hydrogenolysis of the carbonaceous solid.

Figure 4 shows ion currents of hydrocarbon ions observed during H_2^+ ion bombardment on the carbonaceous solid on MS 5A, as a function of bombardment time and temperature. Small

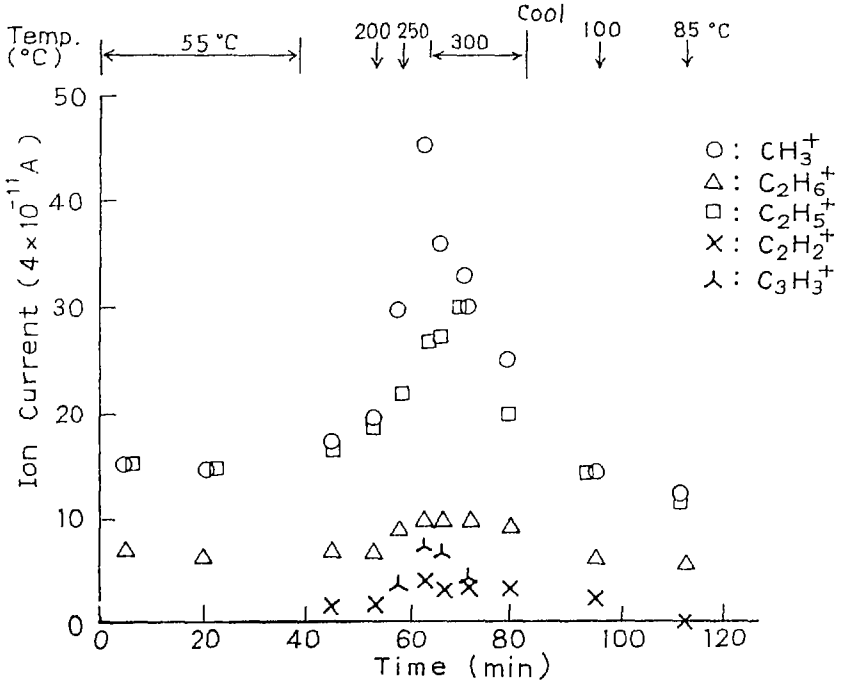

Fig. 3 Ion currents of hydrocarbon ions produced during electron impact under an H_2 atmosphere on carbonaceous solid deposited on MS 5A: electron impact, 3 keV; H_2, 1×10^{-6} Torr.

amounts of methane and ethane were detected at 42°C. The H_2^+ ion bombardment at 300°C resulted in a rapid increase in the concentration of methane and produced small amounts of ethane, propane, ethylene and propylene. Similar results were obtained with the carbonaceous solid on silica gel.

Comparison of Fig. 3 with Fig. 4 reveals that the hydrocarbon products and the temperature dependence of the formation by electron impact under an H_2 atmosphere of the carbonaceous solid on MS 5A are almost the same as those by H_2^+ ion bombardment. Therefore, it may be suggested that H_2^+ ions participate in the radiation-induced hydrogenolysis of the carbonaceous solid.

Table 1 compares the concentrations of methane produced from the carbonaceous solids on MS 5A and on silica gel and

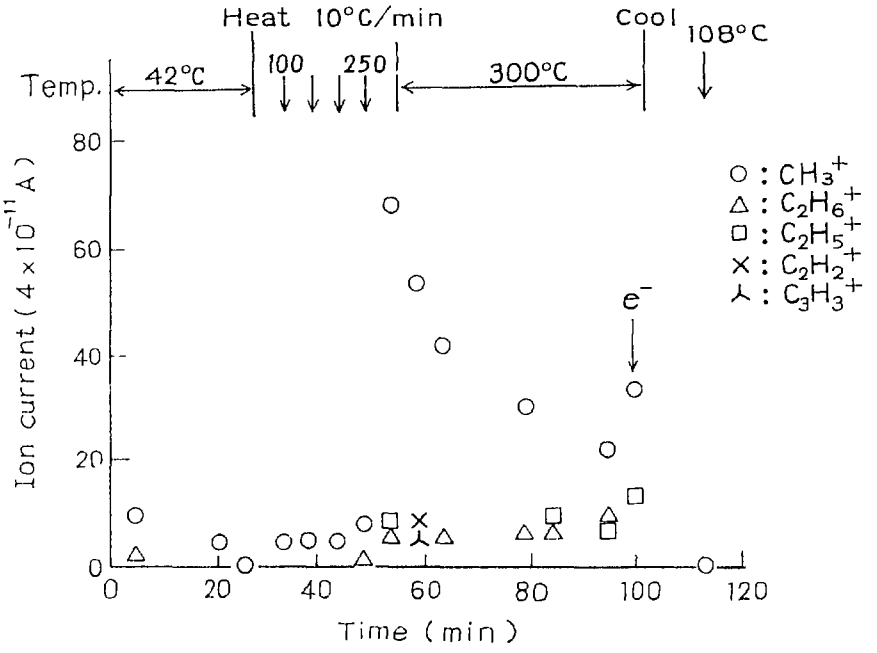

Fig. 4 Ion currents of hydrocarbon ions produced during H_2^+ bombardment on carbonaceous solid deposited on MS 5A: H_2^+ bombardment, 3 keV.

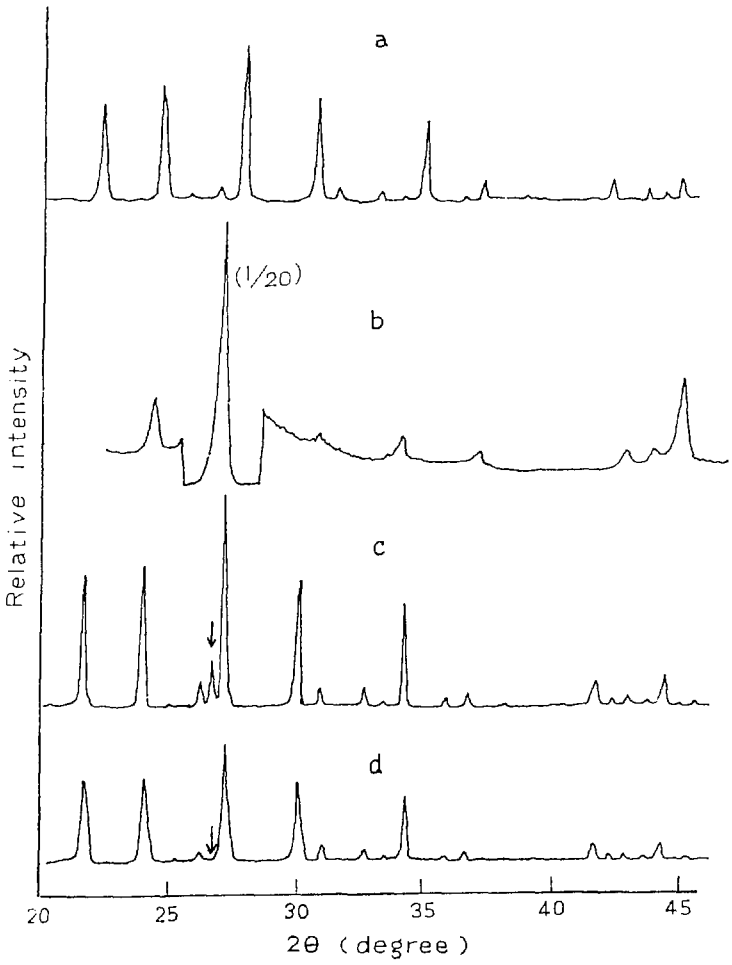

Fig. 5 X-ray diffraction patterns of MS 5A (a), graphite (b), MS 5A (98 wt%) + graphite (2 wt%) mixture (c), and carbonaceous solid on MS 5A (d).

Table 1 Comparison of Methane Yield Produced during Electron Impact under an H_2 Atmosphere and during H_2^+ Bombardment[a)]

Temperature (°C)	C-solid/MS 5A		C-solid/Silica gel		Graphite	
	e^-/H_2	H_2^+	e^-/H_2	H_2^+	e^-/H_2	H_2^+
50	15	9	1	9	4	9
100	16	3	2	6	8	10
150		3		6		10
200	19	3		9	8	10
250	29	6	2	9	9	11
300	45	66	6	12	14	13

a) CH_4 (m/e = 15): $4 \cdot 10^{-11}$ A
Electron impact under an H_2 atmosphere:
3 keV; H_2, 1×10^{-6} Torr
Ion bombardment: H_2^+, 3 keV

graphite observed in these experiments. It can be seen that the concentration of methane produced from the carbonaceous solid on MS 5A at 300°C is greater than that from graphite both during electron impact under an H_2 atmosphere and during H_2^+ ion bombardment, although the carbon content of the sample is much lower than graphite. This result indicates that the carbonaceous solid is more reactive than graphite towards the formation of methane when irradiated with electrons under an H_2 atmosphere or H_2^+ ions. Therefore, it appears that the carbonaceous solid on MS 5A may have an imperfect graphitic carbon structure.

As shown in Fig. 5, X-ray diffraction pattern of the carbonaceous solid on MS 5A (d) does not give the diffraction peak at $2\theta = 26.5°$ corresponding to the interlayer spacing (3.35 Å)[6)] of the graphite crystal structure, which is observed with both graphite (b) and graphite (2 wt%) + MS 5A (98 wt%)

mixture (c). Thus, no evidence was obtained that the carbonaceous solid has the crystal structure of graphite.

(Y. Shimizu and S. Nagai)

1) Y. Shimizu, S. Nagai, and M. Hatada, JAERI-M 83-199, 26 (1983).
2) S. Nagai and Y. Shimizu, JAERI-M 83-199, 40 (1983).
3) S. Nagai, Y. Shimizu, and M. Hatada, JAERI-M 82-192, 29 (1982).
4) J. T. Grant and T. W. Haas, Surf. Sci., 24, 332 (1971).
5) T. W. Haas, J. T. Grant, and G. J. Dooley III, J. Appl. Phys., 43, 1853 (1972).
6) For example, B. T. Kelly, "Physics of Graphite", Applied Science, London, 1981, p. 17.

3. Electron-Beam Recoil Doping of Iron on Silicon or Silica Gel

It was reported that aluminum was injected into silicon through aluminum-silicon boundary by electron irradiation of aluminum sheet in contact with silicon wafer.[1] Studies have been carried out in an attempt to learn whether chemical modification of the solid surface can be achieved by the electron-beam recoil doping method. This year, we selected silicon wafer and silica gel as the surface and iron as the material to be injected to give catalytic activity for Fischer-Tropsch reaction to the surface.

Silicon wafer was a p-type silicon doped with Zn obtained from the Yamanaka Semiconductors Co., and silica gel was of reagent grade supplied by Merck AG. Electron irradiation of the samples was carried out using an electron accelerator of rectifying transformer type at the accelerating voltage of 0.8 MV and beam current of 1 mA for 3600 s under a helium stream containing iron pentacarbonyl in a flow type reaction vessel (FIXCAT-II) made of stainless steel with titanium irradiation window on top. For the purpose of the calibration of depth

distribution of implanted iron, iron ion was injected to silicon wafer by an ion accelerator at the Nissin High Voltage Industries, Ltd. in Kyoto. The accelerating voltage and the amount of iron injected were 30 kV and 5×10^{16} ions/cm^2, and 50 kV and 1×10^{16} ions/cm^2, respectively, and the ion beam current was 7 μA for both cases.

After irradiation with electron beam or injection, the wafer was subjected to surface analysis using an SIMS-Auger System (AES-350S) to observe the change of Auger electron spectrum during Ar^+ sputtering which was carried out at accelerating voltage of 5 kV and source pressure of 4.0 div. Silica gel was pressed to form a disk before the surface analysis.

Catalytic activity of the solid surface to Fischer-Tropsch reaction was examined using a gas flow recycling system composed of a reaction vessel (10 mm in diameter, and 200 mm long), a gas reservoir (7.1 ℓ in capacity), and a gas sampler which automatically injects 1 ml reacting gas from the circulating flow system into a gaschromatograph at a constant repetition period. The reactant gas was a mixture of 1 : 4 by volume of CO and H_2, and the temperature of catalysts was from 150 to 350°C. The content of iron supported on silica gel was determined by calorimetric method.

Figure 1 shows the depth profile obtained from silicon wafer injected with iron at 30 kV. The Auger peaks due to C(KLL) and O(KLL) decreased with sputtering time, whereas Si (KLL) and Si(LMM) signals increased with sputtering, indicating that the surface contaminating material containing C and O were removed by the sputtering. Auger peaks due to Fe(LMM) appeared by 30 minute sputtering, reached a maximum value at 100 min and then decreased with increasing sputtering time. Almost similar depth profile was reported by Thailamani et al.[2] The range R_p of iron ion in silicon wafer is defined as the depth where maximum concentration of iron was found during sputtering and is calculated by a semi-empirical formula by Kalbitzer and Oetzman.[3]

$$R_p = \rho/(\pi a^2 \gamma' N)$$

$$\gamma' = 4M_1M_2/(M_1+M_2)^2$$

$$\rho = 1.967\ \varepsilon^{(2.047+0.420\varepsilon+0.070\varepsilon^2)}$$

$$a = 0.8853\ a_0/(Z_1^{1/2}+Z_2^{1/2})^{2/3}$$

$$\varepsilon = a\ M_2\ T/\{Z_1Z_2\ e^2(M_1+M_2)\}$$

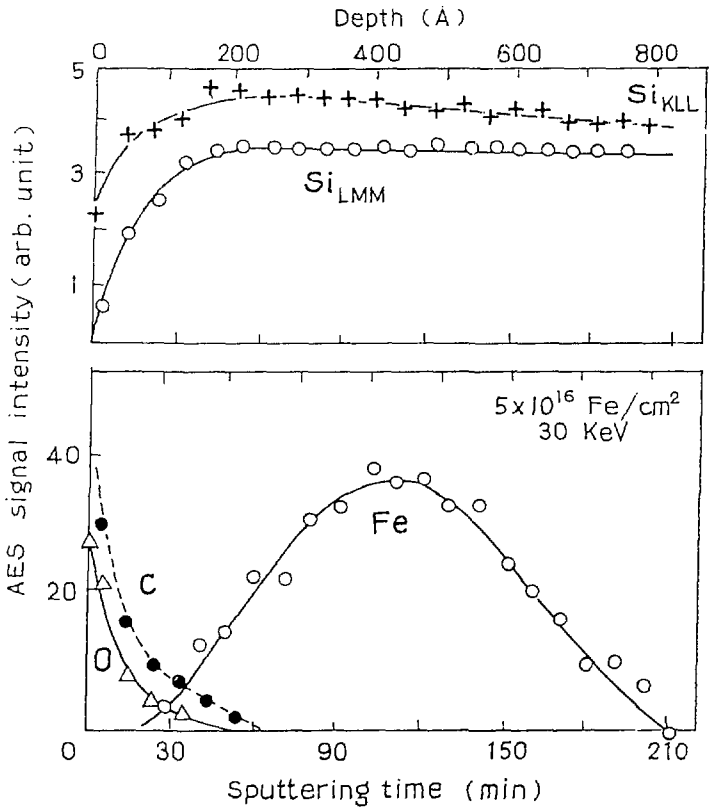

Fig. 1 AES signal intensity as a function of sputtering time for silicon wafer injected with iron ion: ion accelerating voltage, 30 kV; number of injected atoms, 5×10^{16} Fe/cm^2.

Subscripts 1 and 2 denote the quantities related to injecting ion and target material, respectively, and a_0, T, M, and Z are Bohr's radius, energy of injecting ion, mass, and atomic number, respectively. Using this formula, the range was calculated to be 390 A for Fe^+ injected at 30 kV. The sputtering rate was estimated to be 3.39 A/min.

Figure 2 shows depth profile of silicon implanted with

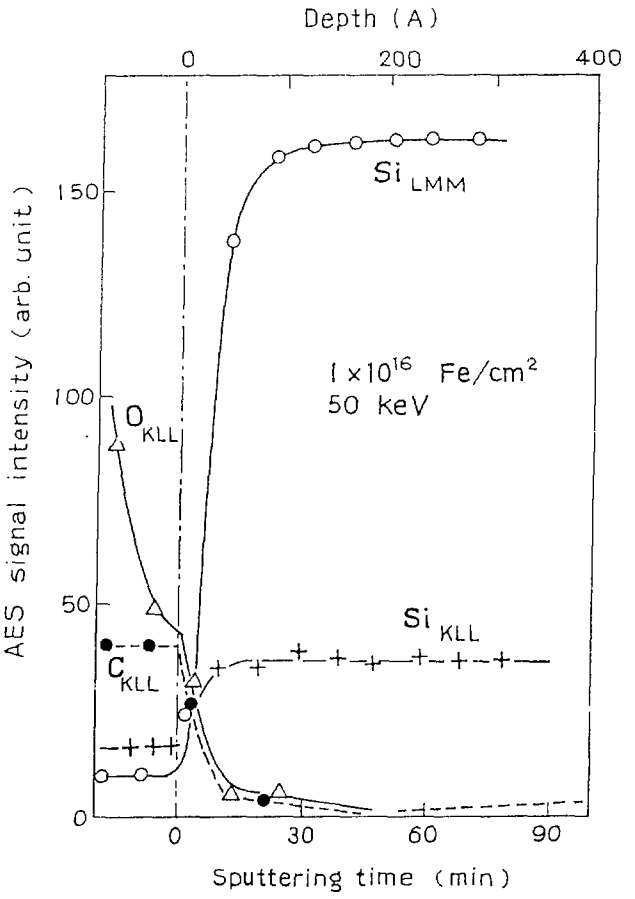

Fig. 2 AES signal intensity as a function of sputtering time for silicon wafer injected with Fe ions: ion accelerating voltage, 50 kV; number of injected iron atoms, 1×10^{16} Fe/cm^2.

iron ion at 50 kV and at 1×10^{17} ions/cm^2. Changes of Si (KLL and LMM), O(KLL) and C(KLL) lines were similar to those observed for the previous experiment, except that no iron signal was detected down to the estimated depth of penetration, indicating that iron atoms in the amount one-fifth of that in the previous experiment are distributed over broader range, and therefore the maximum ion concentration is suppressed below the detection limit. This was confirmed by the calculation mentioned above.

Figure 3 shows the depth profile obtained for silicon wafer on which iron was doped by electron beam irradiation. The Auger lines due to Si(KLL, LMM) increased whereas those due to C(KLL) and O(KLL) decreased during Ar^+ sputtering. The Fe(LMM) peaks also decreased with sputtering time indicating distribution of iron extends up to 300 A or deeper below the surface. The depth giving a half that of the surface concentration is about 120 A. Since the observation of the boundary of the two interface was always accompanied by broadening during

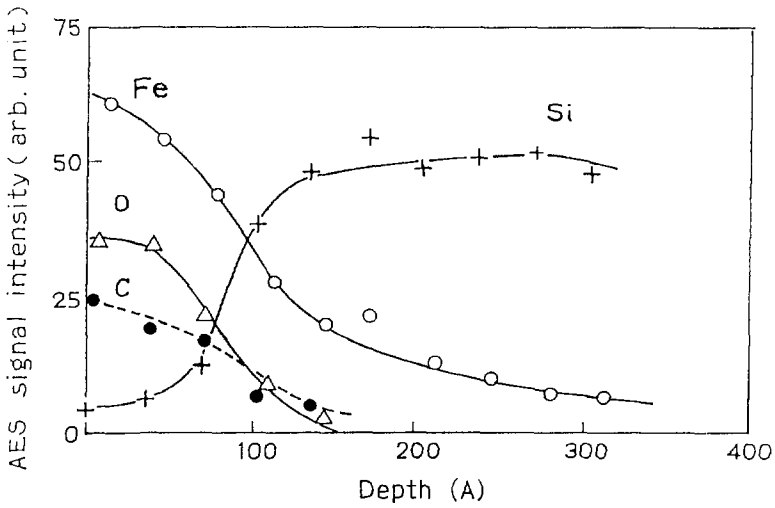

Fig. 3 AES signal intensity as a function of depth for silicon wafer injected with iron by electron beam recoil doping: electron energy, 0.8 MV; beam current, 2 mA.

Table 1 Catalytic Activity for Fischer-Tropsch Reaction

	Irradiated		Blank	
	Yield	Ea (kcal/mole)	Yield	Ea (kcal/mole)
CH_4	0.094	24.9	0.13	18.9
C_2H_4	0.012	22.3	0.004	15.8
C_2H_6	0.015	30.8	0.018	20.2
C_3H_6	0.014	22.5	0.018	17.9
C_3H_8	0.003	25.0	0.011	23.3
$1\text{-}C_4H_8$	0.003	15.7	0.007	13.5
$n\text{-}C_4H_{10}$	0.005	24.0	0.014	19.7

10^{-6} mol(10ℓ reactant)$^{-1}$(mgFe)$^{-1}$(min)$^{-1}$

sputtering, more quantitative conclusion on the depth profile of iron should be derived after a blank experiment without electron irradiation which will be carried out in future studies.

Similar experiments on electron beam injected silica gel surface did not give reproducible profile depending on the position of the electron beam probe due to its rough surface properties but in some spots, iron seems to distribute deeper than non-irradiated reference surface. An example of the results on catalytic activity of Fischer-Tropsch reaction is shown in Table 1 where the rates of hydrocarbon formation normalized to those at unit concentration of iron observed for irradiated surface were smaller for most products except ethane than those observed for non-irradiated reference surface. Larger activation energies of the hydrocarbon formation were obtained on the irradiated surface. The experiments to observe the catalytic activity on flat silicon surfaces both iron ion injected or electron beam injected were not successful due to their small surface area.

(M. Hatada, S. Sugimoto, and S. Nagai)

1) T. Wada, Nucl. Instr. Methods, 182/183, 131 (1981).
2) L. E. Thailamani and M. C. Joshi, Nucl. Instr. Methods, 191, 87 (1981).
3) Kalbitzer and Oetzman, Rad. Effects, 47, 57 (1972).

4. Decrease of Short Circuit Current of AlGaAs/GaAs Solar Cells during Electron Beam Irradiation

Photo-electric conversion efficiency of AlGaAs/GaAs solar cells is known to decrease when they are exposed to high energy radiations in space[1]. It is of interest to know what types of damage effectively result in the decrease of the efficiency and to know a steady state value when extremely large amount of dose is accumulated in the solar cell. The present study has been carried out in an attempt to evaluate dose absorbed by the solar cell considering back scattering from the plate on which they were irradiated, and to measure the short circuit current under simultaneous irradiation of electron and illumination of light from a solar simulator.

Dosimetry of the solar cell was based on the optical density change of CTA film dosimeter which has been calibrated with ionization current in an ionization chamber. For precise evaluation of the dose absorbed by sample which is irradiated on a substrate, it is necessary to make correction of the energy absorption due to the back scattering electrons from the substrate. This correction is important for thin plate like samples on substrates of high Z materials with low incident electron energy. The back scattering coefficient, f, was calculated using an empirical scaling law (1) proposed by Tabata, et al.[2]

$$f = a_1/(1 + a_2 \times T^{a_3}) \qquad (1)$$

where

$$T = T/(mc^2)$$

T : incident electron energy

$a_1 = b_1 \exp(-b_2 Z^{-b_3})$

$a_2 = b_4 + b_5 Z b_6$

$a_3 = b_7 - b_8/Z$

Z : atomic number of the substrate material.

The constants, b_i's are given in Table 1.

Table 1 Values of the constants b_i

Constant	Values
b_1	1.15 ± 0.06
b_2	8.35 ± 0.25
b_3	0.525 ± 0.020
b_4	0.0185 ± 0.0019
b_5	15.7 ± 3.1
b_6	1.59 ± 0.07
b_7	1.56 ± 0.02
b_8	4.42 ± 0.18

Short circuit current of the solar cell was measured on a brass plate which was held horizontally and was cooled by running water in air. The parallel light beam from a Xe lamp was reflected by a thin aluminum foil (0.1 mm in thickness) which was placed above the sample at the angle of 45° with respect to the solar cell surface so that the light beam illuminates perpendicularly on the surface. The spot electron beam of 1.5 MV and 30 μA penetrated through the aluminum foil reflector and reached the cell surface. This experimental set up permits the solar cell surface to be illuminated by light and simultaneously to be irradiated by electron beam.

The intensity of light on the surface was measured by a

calibrated thermopile (Eplay) mounted in place of the sample and was determined to be 33.9 mW/cm^2. The electron dose was determined to be 0.224 Mrad/s as described previously.

The short circuit current was measured during heating and cooling cycles of the solar cell irradiated at 77 K at 200 Mrad to find annealing effect of trap center produced by electron irradiation.

Figure 1 shows the change of short circuit current as a function of dose in logarithmic scales. The short circuit current decreased with dose as reported by Yoshida[3] up to 10^{16} e/cm^2, but it seems that the short circuit current asymptotes to a constant value which is about 40% of the original value.

The short circuit current I_{sc}, is to the diffusion length Le, of electrons in p-region provided that the Le be smaller than the active layer in p-region. Assuming that the number of the trap center of electrons N, increases with increasing dose D, by eq. (2):

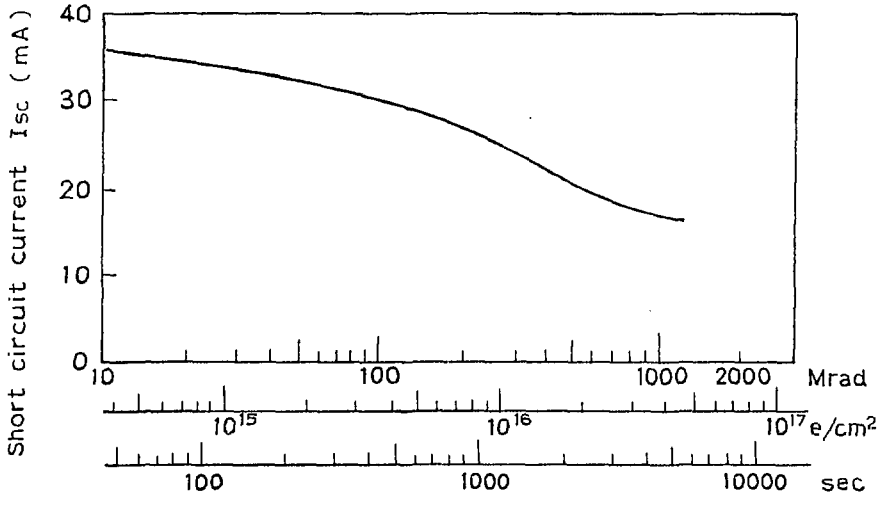

Fig. 1 Short circuit current as a function of dose during simultaneous irradiation with electron and light.

$$N = (N_0 + G\ D/100) \tag{2}$$

where N_0 is the number of trap center originally presented in the layer, the short circuit current is related to eq. (3);

$$I_{sc}^{-2} = A + B\ D \tag{3}$$

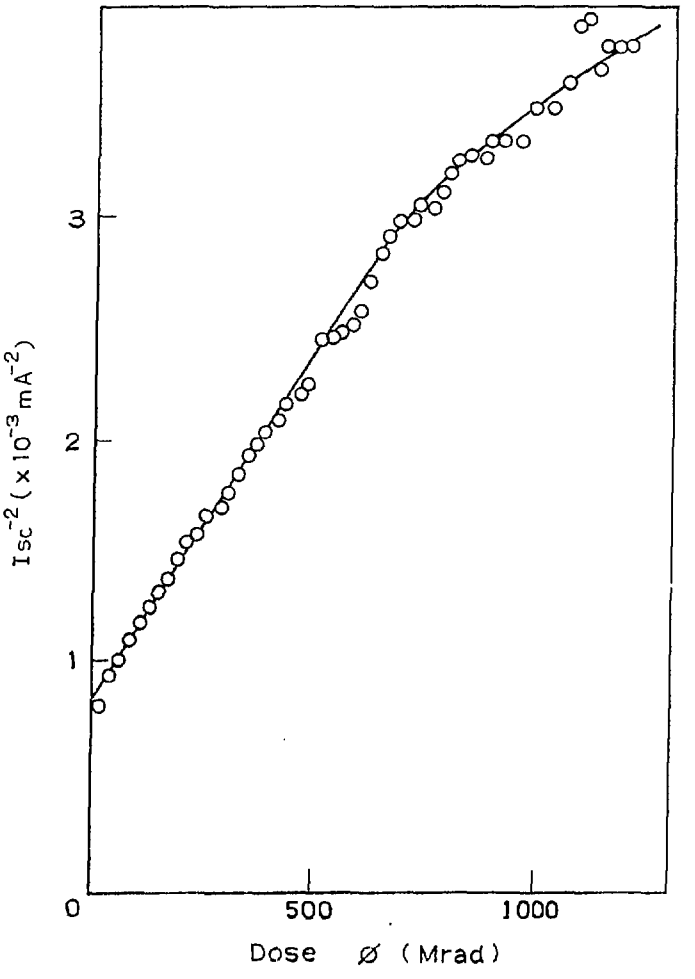

Fig. 2 $(I_{sc})^{-2}$ as a function of dose.

where A and B are constants.

The plot of eq. (3) is shown in Fig. 2 where it is noted that the I_{SC}^{-2} linearly increased up to the dose of 600 Mrad and above this dose, the slope becomes smaller. The results indicate that the diffusion length Le, which is larger than the active layer thickness for the GaAs solar cells, decreased by initial stage of irradiation, and that some of the trap centers are diminished by some interactions between the centers and the numbers of the centers asymptotes to a constant value.

The open circuit voltage of the cell decreased from 0.85 to 0.65 V by the irradiation.

Annealing test of the solar cell irradiated at 77 K revealed that the I_{SC}-temperature curve did not significantly change during repeated cycles of heating and cooling of the sample between 77 and 400 K, exhibiting no evidence for annealing of the trap centers.

(M. Hatada, K. Matsuda and S. Hokuyo)

1) S. M. Sze, Physics of Semiconductor Devices, Wiley-Interscience, 1969.
2) T. Tabata, et al., Nucl. Instr. and Meth., 94, 509 (1971).
3) S. Yoshida, et al., 15th Photovoltatic Specialists Conf., Florida, U.S.A. (1981).

5. Effect of Atmosphere on the Thermoluminescence of Irradiated Polyethylene

In the thermoluminescence glow curves of low density polyethylene irradiated at 77 K in vacuum, there are three peaks at 100, 166 and 250 K as mentioned by Charlesby et al.[1] These peaks are supposed to be due to the trapped electrons at impurity sites or to the migration of charged particles, but no definite explanation is given at present. Most studies[2,3] agree in that the luminescences are observed at the temperatures where the rotation of the terminal groups or the molecular

motion of the main chain occurs (β- or γ-mechanical dispersion).

In an attempt to clarify these three peaks, studies have been carried out on the effect of atmosphere on the thermoluminescence glow curve. Specimens of commercially available polyethylene (Sumikathene) were used as received, after removing additives by Soxhlet extraction with ethanol, or after recrystallization from 0.1% hot xylene solution.

Experimental apparatus for thermoluminescence measurement used in the experiments is schematically shown in Fig. 1. When the sample is irradiated, a concave mirror is removed from the path of the electron beams and after irradiation the mirror is set at the position where the thermoluminescence is allowed to admit to the photomultiplier (EMI 6256B). The photomultiplier output signal was intensified by an amplifier and then was recorded as a function of temperature on an XY recorder to

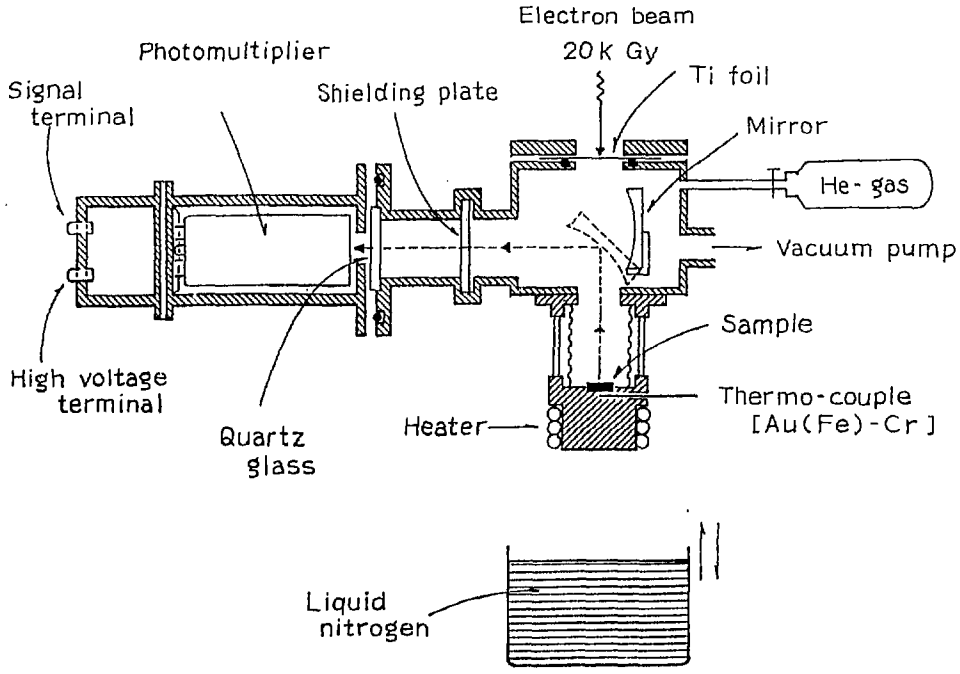

Fig. 1 Experimental apparatus for thermoluminescence measurement.

obtain glow curves.

The specimen sheet (25 mmϕ × 1 mm) was irradiated with electron beams up to the dose of 20 kGy at 77 K and then heated at the constant rate of 10 K/min to observe the thermoluminescence glow curve. An example of the glow curves is shown in Fig. 2. Three peaks at 110, 180 and 250 K in the curves were observed under helium atmosphere at 760 Torr, while the peak at 110 K decreased its intensity as the helium pressure decreased, and completely disappeared under 10^{-3} Torr. Similar phenomenon

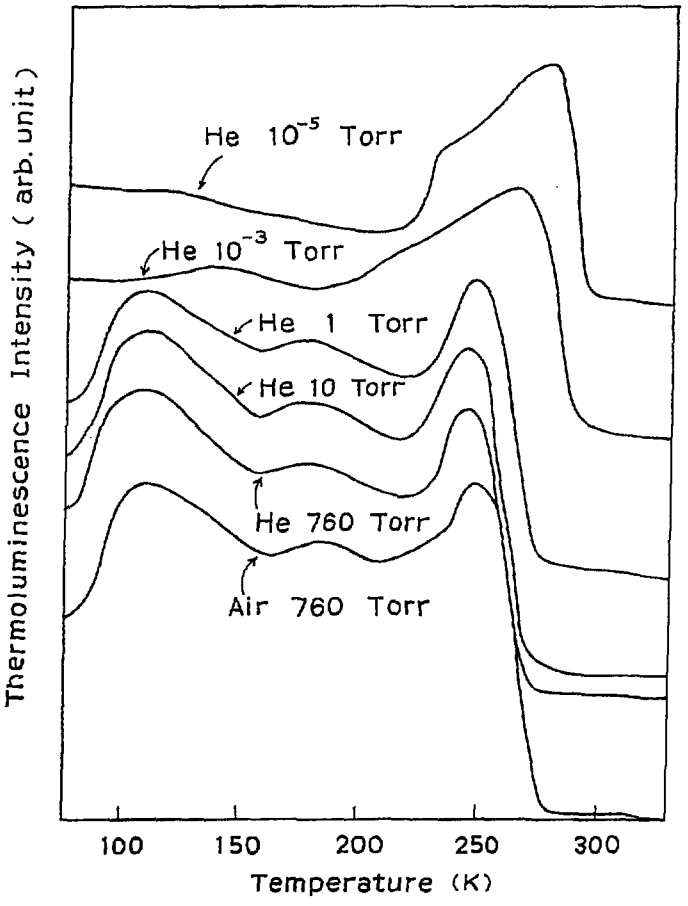

Fig. 2 Pressure dependence of thermoluminescence glow curves of low density polyethylene.

was also observed when hydrogen was used instead of helium. These results indicate that the luminescent center was created by the interaction of matrix substance with excited atmospheric atoms after penetration into the vacancies in the matrix.

In order to examine the effect of impurities on the thermoluminescence glow curve, the experiments were carried out on the specimens which has been purified by the Soxhlet extraction with ethanol at different time.

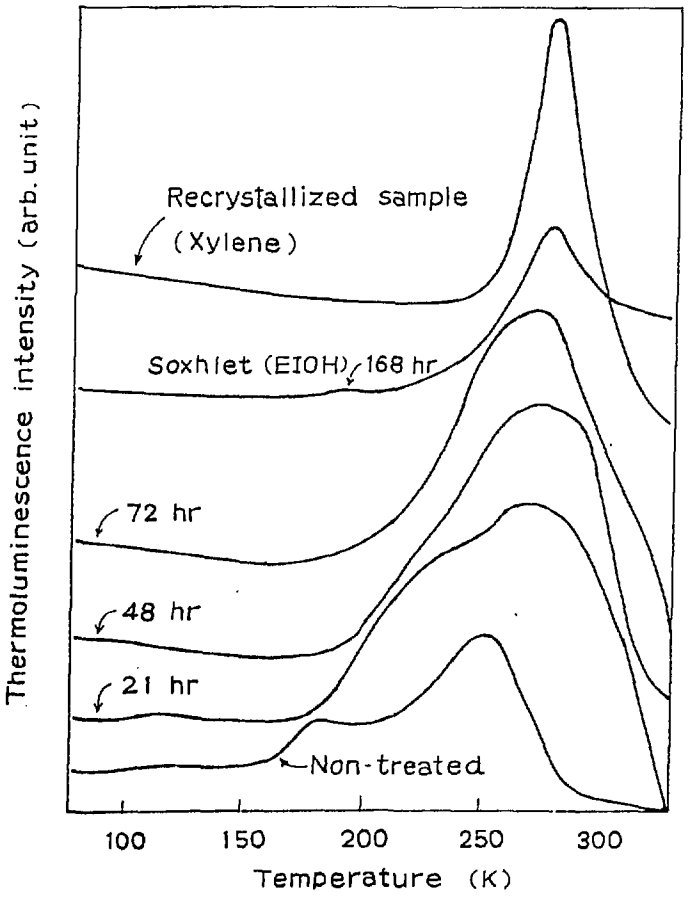

Fig. 3 Effect of impurity on thermoluminescence glow curves of low density polyethylene measured at the pressure of 10^{-5} Torr.

The results shown in Fig. 3 indicate that the peak at 180 K shifted toward higher temperature with increasing the extraction time. The specimen recrystallized from xylene solution exhibits only a sharp peak at 250 K, and no peak at 180 K in the glow curve. It is assumed that the peak at 180 K is influenced by the presence of impurity.

The activation energies estimated for the low temperature (110 K)- and high temperature (250 K)-peaks observed at 760 Torr helium atmosphere were 0.12 and 0.36 eV, respectively. Thus, it is inferred that the peak at 250 K may be resulted from electrons trapped in polyethylene at deep levels which are not affected by the presence of impurity or atmosphere.

(K. Matsuda, Y. Nakase, Y. Tsuji and I. Kuriyama)

1) A. Charlesby et al., Radiat. Phys. Chem., 13, 45 (1979).
2) A. Charlesby et al., Proc. Roy. Soc., 271, 170, 188 (1963).
3) L. Y. Zlatkevich et al., J. Polym. Sci., 19, 1177 (1981).

6. Preparation of Thin Polymer Films by Electron Beam Induced Polymerization of Styrene Vapor

Studies have been carried out in an attempt to prepare thin polymer film by electron beam irradiation of styrene vapor. Styrene (liquid) was poured into a reaction vessel (Fig. 1) made of Pyrex glass containing a Teflon coated magnetic stirrer at the bottom. A pyrex glass substrate (1 mm thick) on which a thin polymer film is to be developed was held horizontally above the liquid surface. The contents of the reaction vessel are separated from atmospheric air by a thin aluminum foil (30 μ in thick) on top, through which an electron beam penetrates into the vessel. No special effort was made to remove air that may be present in the liquid or vapor phase in the vessel.

The vapor pressure was 360 Torr and dose rate, 8.0×10^4 rad/s.

After irradiation, polymer mist in vapor phase taken out by a cyringe, polymer formed on the glass substrate and liquid phase were placed in a vacuum desiccator to remove unreacted

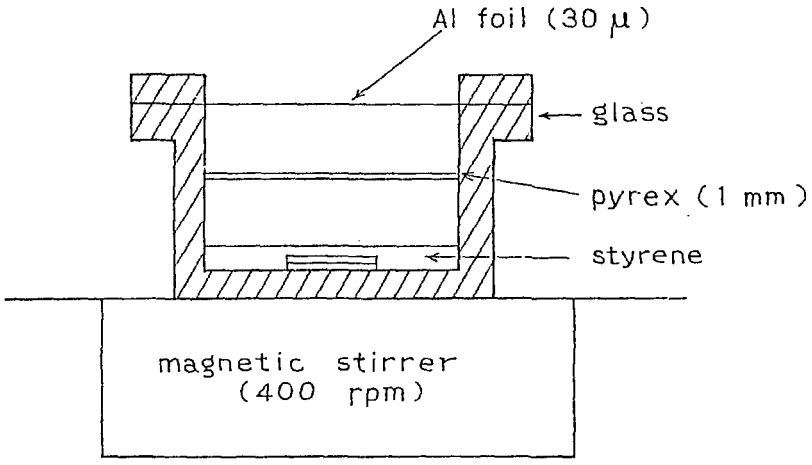

Fig. 1 Irradiation apparatus.

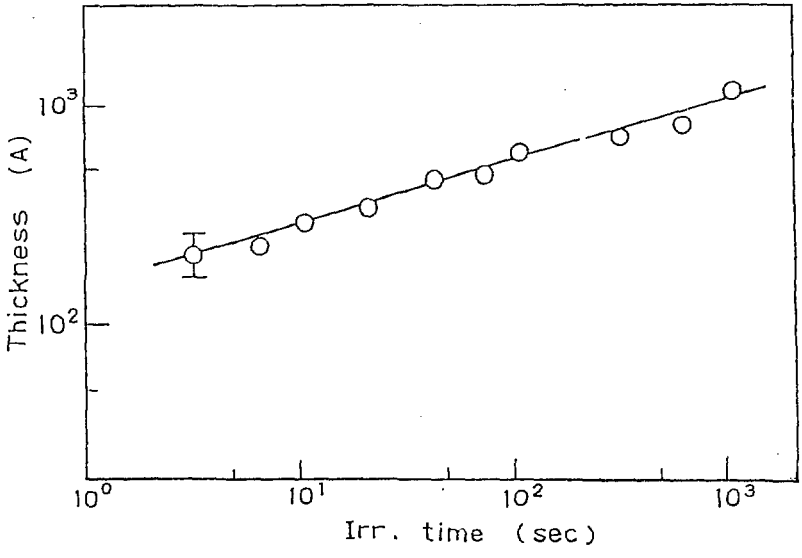

Fig. 2 Tickness of polymer film as a function of irradiation time.

monomer, and then subjected to GPC separately for the determination of molecular weight distribution. The thickness of the polymer film on the glass substrate was measured by an interferometric microscope.

The thickness of polymer film was plotted as a function of irradiation time in logarithmic scales as shown in Fig. 2, in which the thickness was found to increase by 0.3 power of irradiation time.

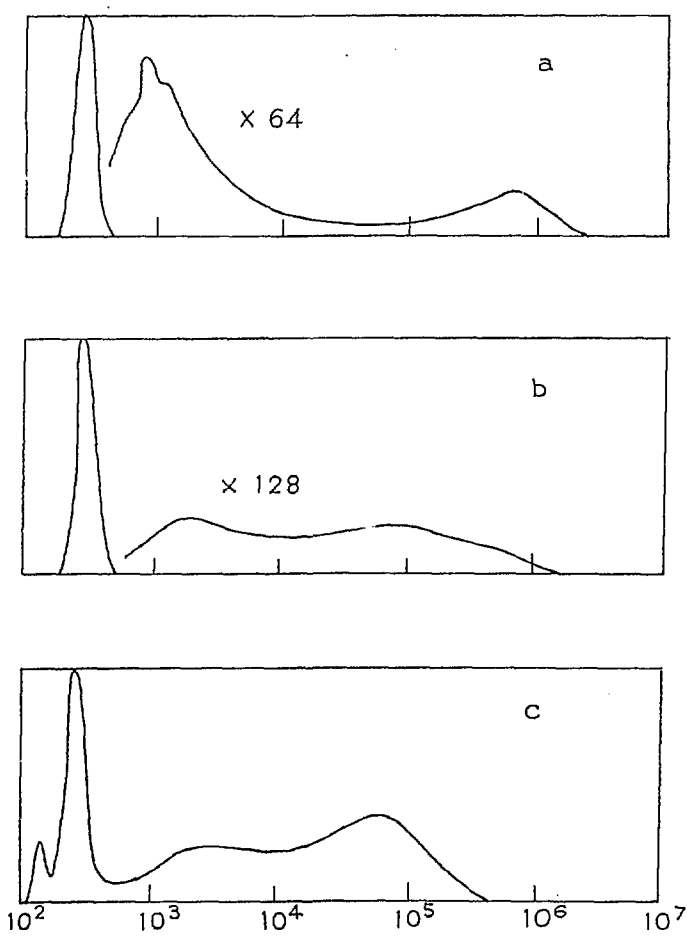

Fig. 3 Molecular weight distribution: (a) thin layer, (b) gas phase, and (c) liquid phase.

Molecular weight distributions of the products are shown in Figs. 3a, b, and c, in which a, recovered from thin layer (after 10 second irradiation), b, from vapor phase, and c, from liquid phase, respectively. The peaks of trimer and of higher degrees of polymerization appear in the GPC obtained for the products of all sources. The amount of high molecular weight fraction is found larger in the product recovered from the liquid phase while it is smaller in the products from thin layer and also vapor phase, suggesting that the propagating step may be somehow restricted at the boundary of the phase in the latter two case.

In Fig. 4, the weight percents of trimer were plotted as a function of irradiation time. The weight percents of trimer in the products from thin layer and vapor phase were found to be above 90% and almost independent of irradiation time until at the point of sharp decrease of the weight percent of trimer. This point was observed at 100 sec for the product from vapor

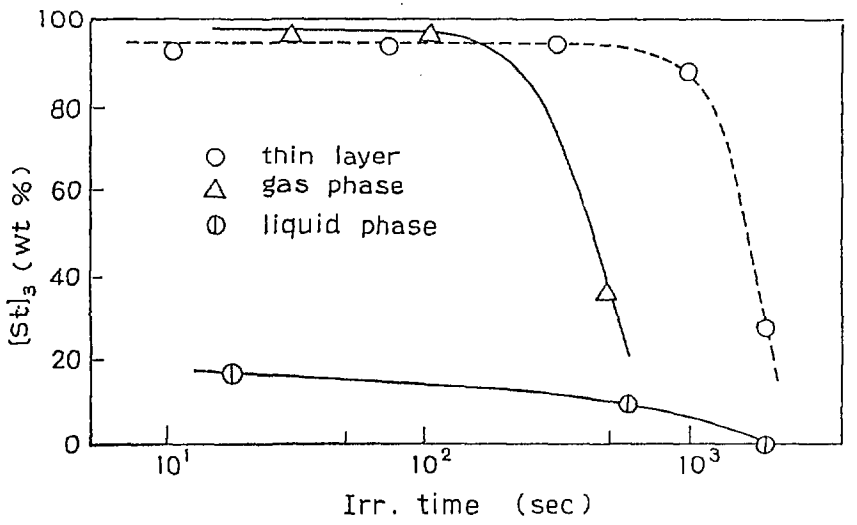

Fig. 4 Weight percent of styrene trimer as function of time: (○) thin layer, (△) gas phase, and (◐) liquid phase.

phase and at later period of time for that from thin layer.

The weight percent of trimer also was observed to be small as 20% for liquid phase and decreased gradually during irradiation.

(J. Takezaki)

7. An Apparatus for Irradiation-Induced Thin Film Polymerization in Gas Phase

Formation of a thin film on a substrate leads to important applications in the electronic technology. Only a few papers hitherto appeared phenomenological observations on the electron beam induced crosslinking of adsorbed silicon oil[1], on the polymerization of butadiene gas[2] in which the rate was followed by a piezoelectric quartz crystal oscillator vacuum microbalance, and electrical properties vs. bombarding currents were investigated at about 150 Å thickness of thin films[3]. Approaches to the mathematical treatment of thin film deposition from gas phase by beam induced polymerization of divinyl benzene were reported with some experimental results[4].

The mechanism of the polymerization has not been clarified yet, so we have carried out the investigation of radiation-induced thin film polymerization by using a crystal oscillator microbalance. Recent development of electronics technique and analytical measurement for the surface enables us to get more detailed informations about the polymerization mechanism.

The film formation with proper properties has to be clarified basically in order to find the way for application of the radiation-induced polymerization for industry.

The experiments were performed in a batch system where the pressure of the monomeric gases, acetylene and butadiene, was maintained constant. In a flow system in the cases of styrene and phenylacetylene the pressure was also kept constant in the irradiation vessel under a nitrogen gas flow (about 1 ℓ/min).

The irradaition was performed using ^{60}Co γ-rays. The rate of polymerization was followed by a crystal oscillator. Small

changes in the total vibrating mass of the oscillator caused a proportional change in the shear oscillation which could be measured accurately.

A sensor with a crystal oscillator was placed at almost the center of the irradiation vessel. The changes of the shear oscillation were converted to the rate of polymerization and the thickness of polymer formed. The absolute values of the

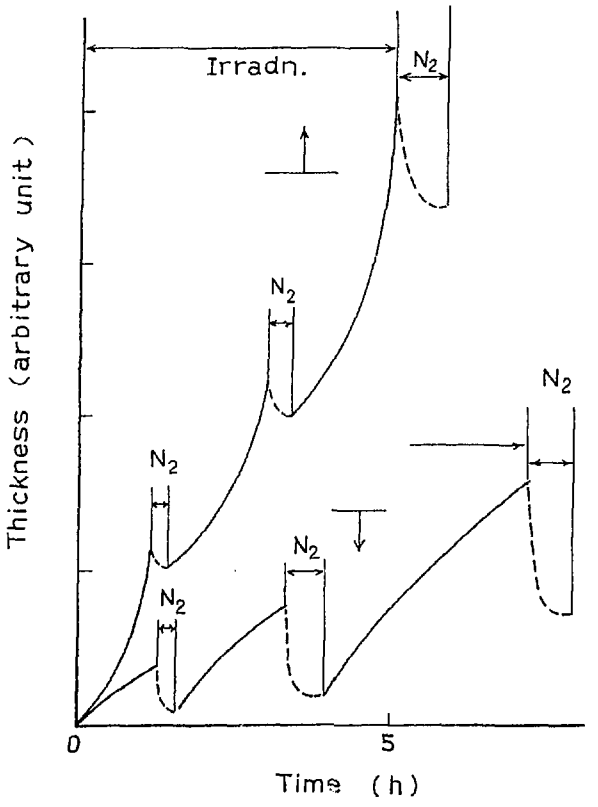

Fig. 1 Relationship between thickness and irradiation time of phenylacetylene in the gas-phase polymerization: dose rate, 0.2 Mrad/h; polymerization temperature, 10°C. ⊥ indicates the surface of the crystal directed to the up-side, and ⊤ directed to the down-side. N_2 indicates the nitrogen gas passed through the vessel (ca. 30 ℓ/min).

thickness were not calibrated yet, and the values were presented at arbitrary unit. The crystal oscillator on the sensor was 12 mm dia. and coated with Ag and it was adjusted to be 5 MHz frequency.

Figure 1 shows the thickness of the polymer film formed on the crystal by the radiation-induced polymerization of phenylacetylene in the gas phase. When the nitrogen gas flow was increased to about 30 ℓ/min, the thickness decreased suddenly to a certain value, denoted as N_2 in Fig. 1, even under irradiation. These results were observed in both cases of the up-side setting (crystal surface was up-side denoted as $\perp$ in Fig. 1) and the down-side setting ($\top$ in Fig. 1). The difference of thickness of the films between two settings suggests the fall-out of particles formed in the gas phase on the surface of the crystal. It is not clear at present whether the particles in the gas phase contain polymer or not. It seems likely that the polymerization takes place in the particles after the fall-out on the surface, since it has been noticed that the thickness observed under no-irradiation was reduced to zero under a higher flow rate of nitrogen gas.

Figure 2 shows the infrared spectrum of the polyphenylacetylene formed on the crystal. The spectrum suggests the presence of cis-type polymer chain and also the easiness of auto-oxidation in the atmospheric circumstance.

Figure 3 shows the thickness of the polymer film formed on the cyrstal under irradiation in the case of styrene. Similar tendency as in the case of phenylacetylene was observed in the polymerization behavior of styrene. The interval of the higher rate of nitrogen gas flow was elongated, the increase of the thickness was larger than that in the case of short interval, indicating the acceleration of polymer formation.

Figure 4 shows the thickness change of polymer film on the crystal with the irradiation time in the cases of gaseous monomer, acetylene and butadiene. After a fixed irradiation time, the monomer gas was passed through with the rate of about 30 ℓ/min as indicated 'Blow' in Fig. 4, then the thickness decreased rapidly to a limited value which corresponded to the

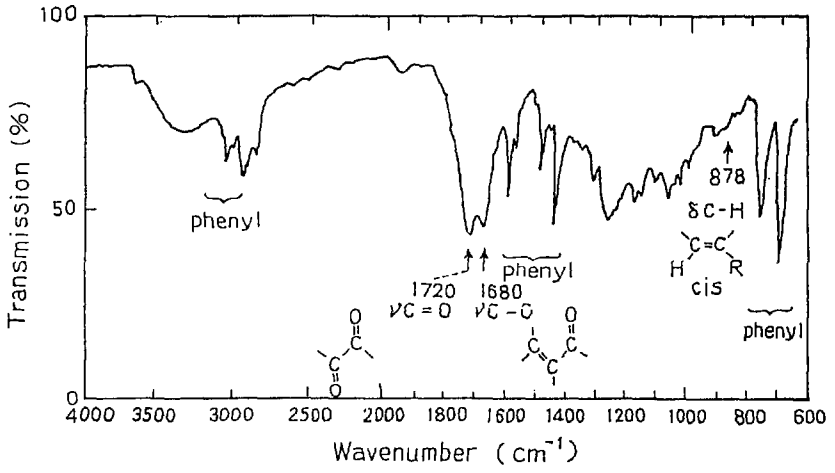

Fig. 2 Infrared spectrum of the polymer deposited on the crystal from gaseous phenylacetylene by gamma-irradiation.

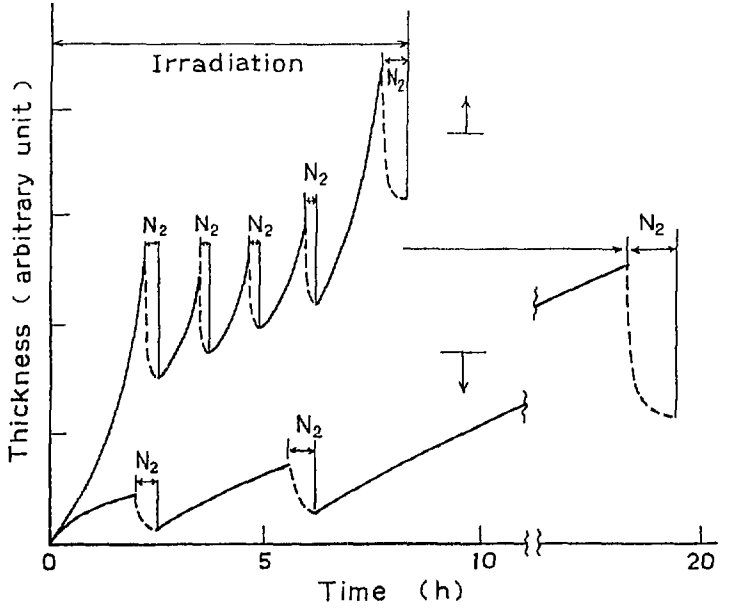

Fig. 3 Relationship between thickness and irradiation time of styrene in the gas-phase polymerization: dose rate, 0.2 Mrad/h; polymerization temperature, 10°C.

polymer thickness.

In the case of no-irradiation, the thickness increase is limited in both cases of acetylene (A) and butadiene (B) in Fig. 4, and the value reduced to zero by 'Blow'.

These results suggest that small amounts of monomer deposited on the crystal are polymerized by irradiation, and then the polymer formed absorbs monomer molecules in the gas phase to form polymer molecules by irradiation. Such a process can take place remarkably in the gas-phase polymerization of acetylene and butadiene.

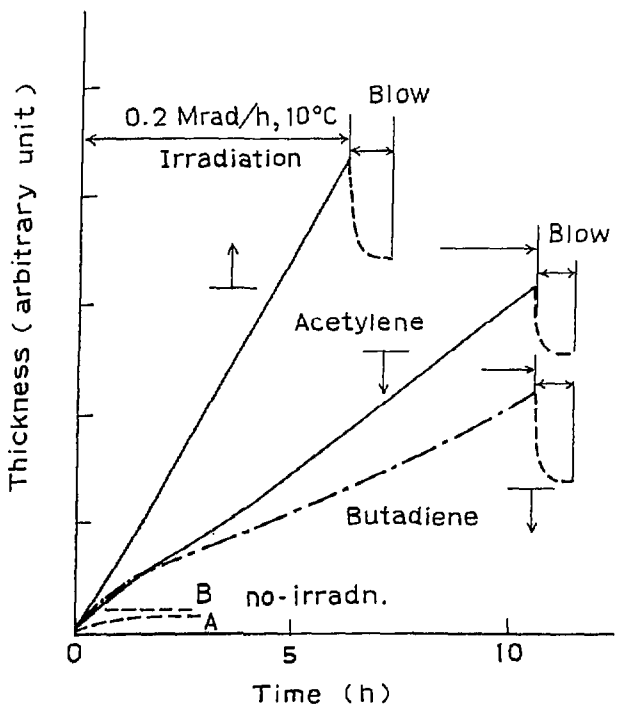

Fig. 4 Relationship between thickness and irradiation time of acetylene and butadiene: dose rate, 0.2 Mrad/h; polymerization temperature, 10°C. 'Blow' indicates the passage of monomeric gas with high flow rate (ca. 30 ℓ/min).

Table 1 Comparison of Polymerization Rates of Four Monomers. The rates are expressed as relative rate taking unity of polymerization rate of styrene. $\perp$ indicates the surface of crystal directed to the up-side and $\top$ directed to the down-side. In the case of the up-side, the polymerization rate is about ten times higher than the case of the down-side.

Monomer	Relative rate ($wt/cm^{-2} \cdot Mrad^{-1}$)	
	$\perp$ × 10	$\top$ × 1
Styrene	1	1
Phenylacetylene	1 ∿ 2	1.5
Acetylene	0.5	2.5
Butadiene	-	1.5

Table 1 shows the comparison of polymerization rate of four monomers used. The polymerization rates were calculated from the thickness obtained, the surface area of the crystal, and specific density of monomers. The relative rates were tabulated taking the polymerization rate of styrene as unity. It is noticed that phenylacetylene may be polymerizaed faster than that of the case of styrene in the particle formed in the gas phase, and also that acetylene polymerizes rather faster than the case of styrene on the surface of the crystal.

The polymerization apparatus constructed and used here, is rather useful to investigate on the radiation-induced thin film polymerization. However, a few problems are left such as the calibration of crystal, the separation of unreacted monomer from the polymer film formed on the crystal. It is also some problems to characterize the polymer film obtained, because of its small amounts in weight and size.

Characterization of polymer obtained seems to be important in order to clarify the difference of thin film polymerization from normal bulk polymerization. Further studies are now

undergoing.

(Y. Nakase and M. Nishii)

1) R. W. Christy, J. Appl. Phys., 31, 1680 (1960).
2) I. Haller and P. White, J. Phys. Chem., 67, 1784 (1963).
3) L. E. Babcock and R. W. Christy, J. Appl. Phys., 43, 1423 (1972).
4) C. R. Fritzsche, J. Appl. Phys., 53, 9053 (1982).

8. Radiation-Induced Polymerization of Phenylacetylene in Condensed Phase

Recent studies to prepare polymers having conjugated double bonds in main chain from acetylene or its derivatives have attracted interest because the polymer doped with electron acceptor shows electric conductivity or semi-conductivity. The polymers were synthesized using Ziegler-catalysts, but only a few reports were concerned with the radiation-induced polymerization of acetylenic compounds in condensed phase[1-3] and the structure of the polymer has not been studied yet. We reported that the γ-rays irradiation of acetylene at -95°C in plastic cyrystalline state gives polyacetylene having linear trans form which is not obtained by other phases.[4] Here, we have studied the radiation-induced polymerization of phenylacetylene in condensed phase and examined the structure of the polymer thus obtained.

The monomer was dried over calcium hydride and then distilled under reduced pressure in a nitrogen atmosphere. The fraction distilled out at 55°C in 35 Torr was further dried and deaerated over calcium hydride, sealed in a glass ampoule in vacuo, and then irrdiated with γ-rays. After irradiation, unreacted monomer was removed by evaporation in vacuo, and the residual was weighed as the polymeric products.

The amount of polymer increased linearly with irradiation time at 25°, 0°, or -23°C (liquid phase above this temperature), or at -72°C (solid phase). The conversion of the polymer was

7% by 50 Mrad irradiation at 25°C where the maximum rate of polymerization was attained. Figure 1 shows the Arrhenius-plot of the rate of polymerization which was calculated based on the data taken in the dose range below 20 Mrad, where the amount of polymer increased linearly with dose. The activation energy calculated from the Arrhenius-plot was 0.74 kcal/mole which suggests that the polymerization proceeds with an ionic mechanism. This is further supported by the result that the rate of polymerization is proportional to 0.97 th power of dose rate in the dose rate range of $0.40 \sim 8.58 \times 10^5$ R/hr.

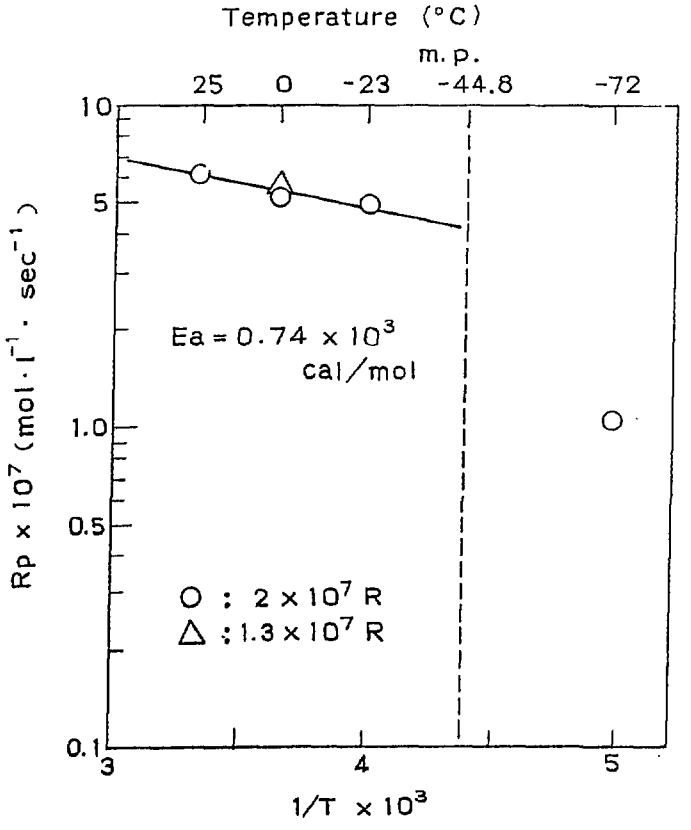

Fig. 1 Arrhenius plots of the polymerization of phenylacetylene.

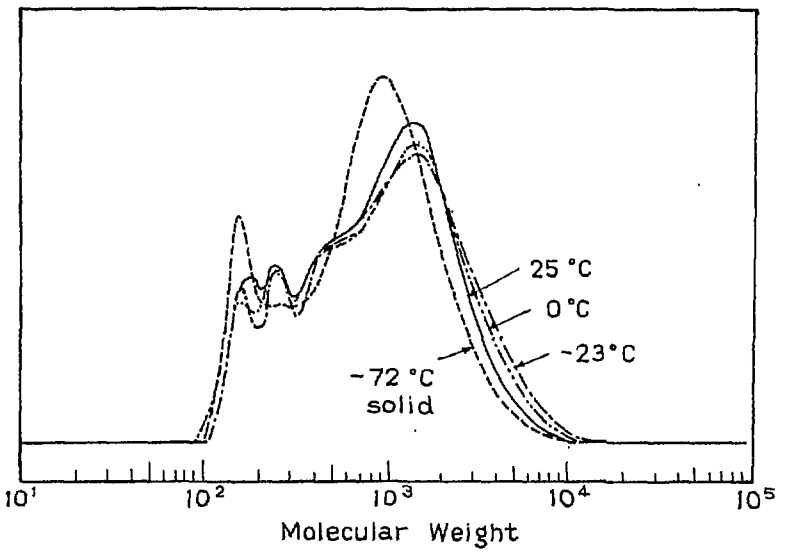

Fig. 2 Molecular weight distribution curves of polyphenylacetylenes obtained at different temperatures.

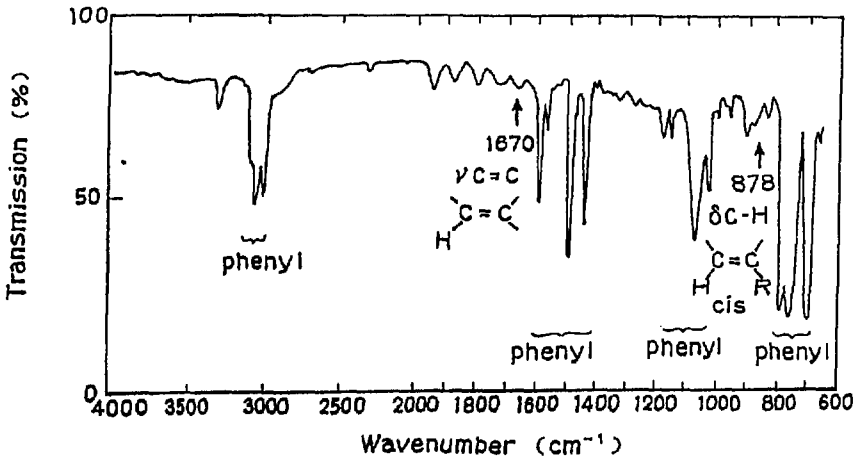

Fig. 3 Infrared spectrum of polyphenylacetylene obtained at 25°C.

The polymer thus obtained was dark-red solid and was soluble in benzene, chloroform, carbon tetrachloride, and tetrahydrofuran, and partly soluble in methanol, but insoluble in n-hexane.

Molecular weight distribution curves obtained by GPC method using tetrahydrofuran as a solvent are shown in Figure 2 where it is noted that a maximum appears at around Mn = 1400, and the molecular weight distribution curves of the polymers obtained at different temperatures are similar one another. It is also noted that the number average molecular weight is smaller for the polymer obtained in solid phase than that obtained in liquid phase. The Mn and Mw/Mn of the polymer obtained at 25°C and purified by precipitation with methanol are 1420 and 1.5, respectively.

The infrared spectrum of the polymer obtained at 25°C is shown in Fig. 3, where absorption bands due to phenyl group appear at 3080, 3060, 3027, 1597, 1572, 1490, 1441, 1154, 1069, 1028, 755 and 693 cm^{-1}. The bands at 1670 and 878 cm^{-1} are assigned to stretching vibration of C=C bond of $\overset{R}{\underset{H}{\diagdown}}C=C\overset{R'}{\underset{R''}{\diagup}}$ group and out-of-plane deformation vibration of C-H bond of cis-C=C group, respectively. Since the strong band due to cis-C=C group at 878 cm^{-1} and lack of the band ($\sim$980 cm^{-1}) due to C-H bond of trans-C=C group are reported for the infrared spectrum of the polymer obtained by catalytic polymerization[5,6], the spectrum of the polymers obtained in the present study seems to indicate that the main chain of the polymer contains more trans structure than that obtained by catalytic polymerization.

In an attempt to reveal the type of intermediates of the polymerization, the polymerization studies were carried out in the presence of 5 $\sim$ 50 mole% of additives: triethylamine and tetrahydrofuran as cation scavengers, and n-butyl chloride as an electron acceptor. However, no definite conclusion was obtained by this experiment on the nature of the intermediates, because none of the additives inhibited the polymerization, but, instead, these additives promoted the polymerization slightly.

(M. Nishii)

1) Y. Tabata, B. Saito, H. Shibano, H. Sobue, and K. Oshima, Makromol. Chem., 76, 89 (1964).
2) I. M. Barkalov, et al., Polym. Sci. USSR, 3, 246 (1962).
3) S. Okamura, K. Hayashi, M. Yamamoto, and Y. Nakamura, Kogyo Kagaku Zasshi, 65, 728 (1962).
4) M. Nishii, K. Hayashi, I. Kuriyama, and S. Okamura, Rept. on Progress in Polym. Phys. in Japan, 26, 555 (1983).
5) Khr. Simionescu, et al., Polym. Sci. USSR, 16, 911 (1974).
6) R. J. Kern, J. Polym. Sci., A-1, 7, 621 (1969).

9. Graft Polymerization of Acrylic Acid onto Polyethylene Film by Preirradiation Method

The purpose of this study is to examine reaction kinetics of the low-temperature grafting of acrylic acid on high density polyethylene (PE) pre-irradiated in air and to know surface structure of the graft PE film. The study is of fundamental interst in preparation of thin grafted layer on polymer surface because the rate of grafting and the morphology of the grafted surface are expected to be dependent on the surface structure of the polymer to be grafted, and also on the reaction conditions employed. The post polymerization technique was used in the present study to avoid the formation of homopolymer.

High density PE film 75 μm thick with a density of 0.944 g/cm^3 was used as a trunk polymer. The film purified by Soxhlet extraction with methanol for more than 8h was irradiated with γ-rays from ^{60}Co at ambient temperature (15°C). Irradiated PE film and acrylic acid aqueous solution were charged into a glass ampoule. After bubbling nitrogen gas (through the solution) for 2 min, the ampoule was sealed and grafting was carried out at constant temperatures from 20° to 60°C. The film after grafting was washed with cold water and soaked in water at 50°C for several hours. Further extraction was done by using an ultrasonic cleaner. Then it was dried at 50°C at a reduced

pressure and weighed. The apparent graft percent was calculated from the weight increase of the film.

In the previous study of grafting of acrylic acid onto polyester[1], poly(vinyl chloride)[2] and polyethylene fiber[3] with a direct irradiation method, addition of metallic salt such as Mohr's salt in monomer solution was successful to prevent homopolymerization outside the fiber. In this study, however, most of experiments were carried out without addition of metallic salt, because the amount of homopolymer in the case of pre-irradiation method is known to be lower than in the case

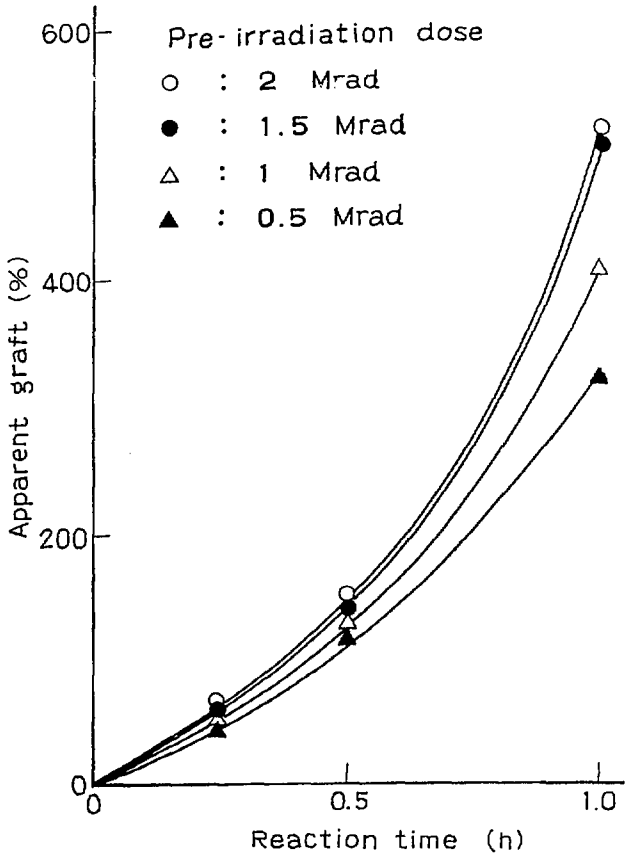

Fig. 1 Effect of reaction time on the grafting: reaction temperature, 40°C.

of direct irradiation method.

Figure 1 shows the plots of degree of grafting at 40°C as a function of reaction time for pre-irradiation doses of 0.5, 1, 1.5 and 2 Mrad, respectively. Grafting is accelearted with increasing reaction time and a few hundreds percent graft was attained in an hour even for a pre-irradiation dose of 0.5 Mrad. We could detect a considerable amount of free radicals in the irradiated PE, but these radicals were found to be distributed throughout the polymer film. The radicals on the surface were

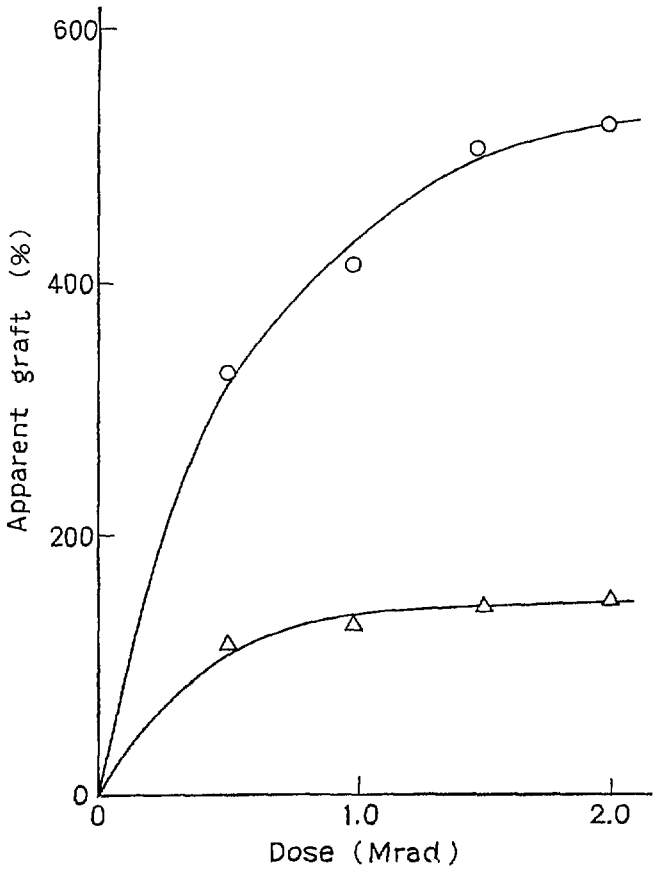

Fig. 2 Effect of dose on the grafting: reaction temperature, 40°C; reaction time, (○) 1 hr, (△) 0.5 h.

supposedly converted to peroxide by the irradiation in air. Since the reaction temperature (40°C) is not high enough for the peroxides to be decomposed and to initiate graft reaction, we might have to assume that the grafting is initiated by the radicals, migrated out from crystalline regions where radicals are trapped. Once the grafting is initiated on the film surface of PE, the fresh PE surface in contact with AA grafted layer is swollen by AA which penetrated through grafted AA layer and therefore, more and more radicals trapped inside the

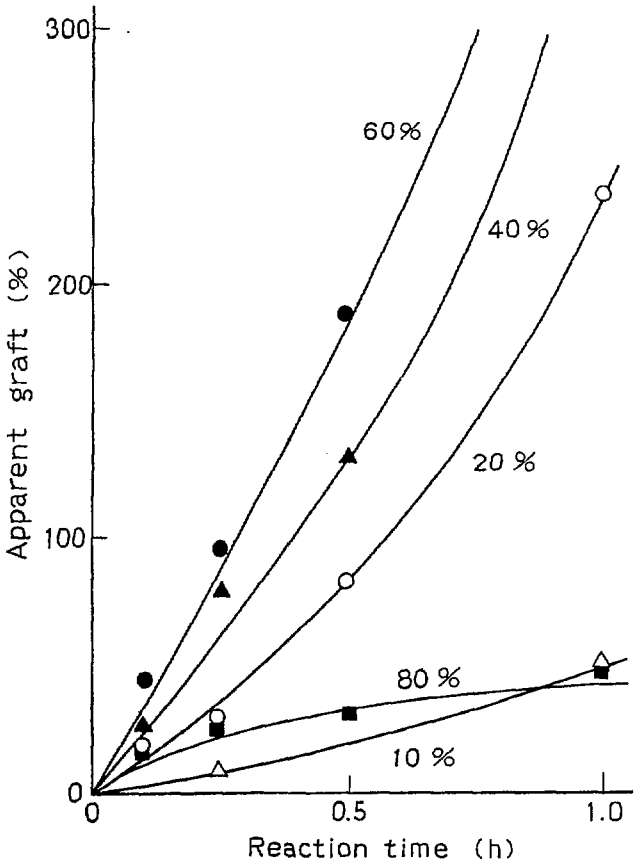

Fig. 3 Effect of monomer concentration on the grafting: pre-irradiation dose, 1 Mrad; reaction temperature, 40°C.

PE film will react to accelerate the grafting of AA.[4]

Figure 2 shows degree of grafting as a function of pre-irradiation dose at two different reaction times. Both curves show that the degree of grafting seems to level-off as the dose increases, but the dose at which the grafting levels off is higher for the longer reaction time, possibly supporting the above assumption that the radicals trapped inside the film contribute to the grafting as the film is swollen by AA aqueous solution.

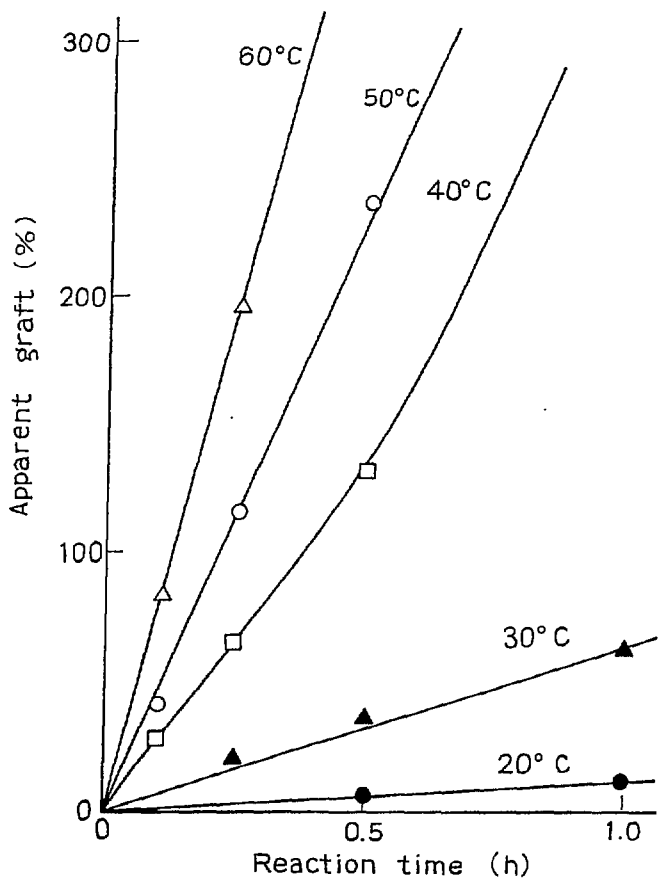

Fig. 4 Effect of reaction temperature on the grafting: pre-irradiation dose, 1 Mrad.

The degree of grafting is plotted in Fig. 3 as a function of reaction time at different concentrations of AA monomer. The rate of grafting increased as the AA concentration increased up to 60% of monomer concentration and the grafting reactions were accelerated with increasing reaction time, whereas at 80% of monomer concentration, the rate was much lower than that obtained at 60% and the grafting reaction levelled-off with increasing reaction time. The results seems again to be explained by the swelling of interfacial region between AA grafted layer and non-grafted PE, because the degree of swelling by poly(acrylic acid) graft PE is known to increase with

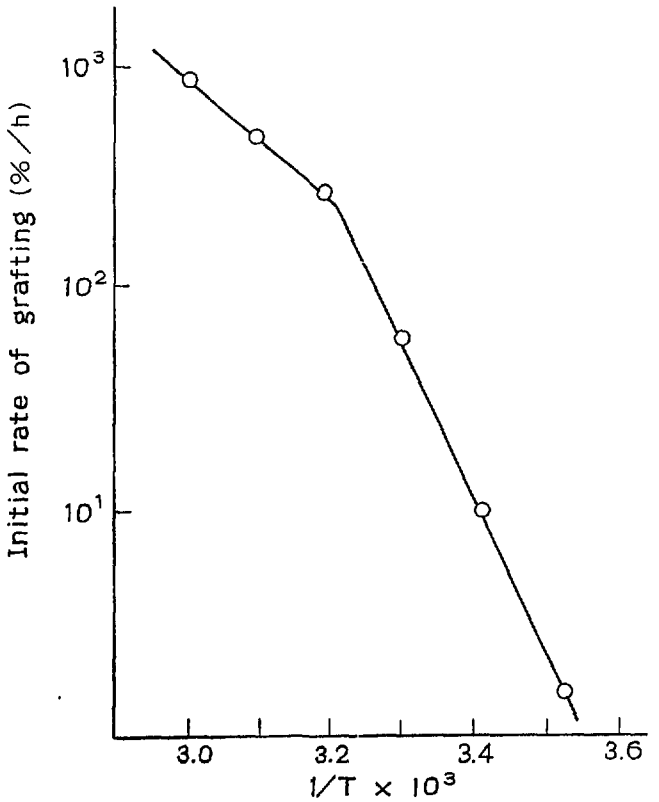

Fig. 5 Arrhenius plot of the initial rate of grafting: pre-irradiation dose: 1 Mrad.

increasing content of AA in the monomer solution, but above 60% of AA content, it decreases with increasing AA concentration[4], perhaps by decreasing of water contents.

Figure 4 shows the degree of grafting as a function of reaction time of different temperature. It is apparent that the rate of grafting increases with the reaction temperature. The Arrhenius plot for the data of Fig. 4 is given in Fig. 5; a bending point appears at 38°C, the activation energies above and below this temperature being 12 and 39 kcal/mol, respectively. The former value agrees with the activation energy for abstraction of hydrogens, e.g., 12 kcal/mol[5], whereas the latter value corresponds to the activation energy for the crystalline relaxation process (α_c), e.g., 42 kcal/mol for

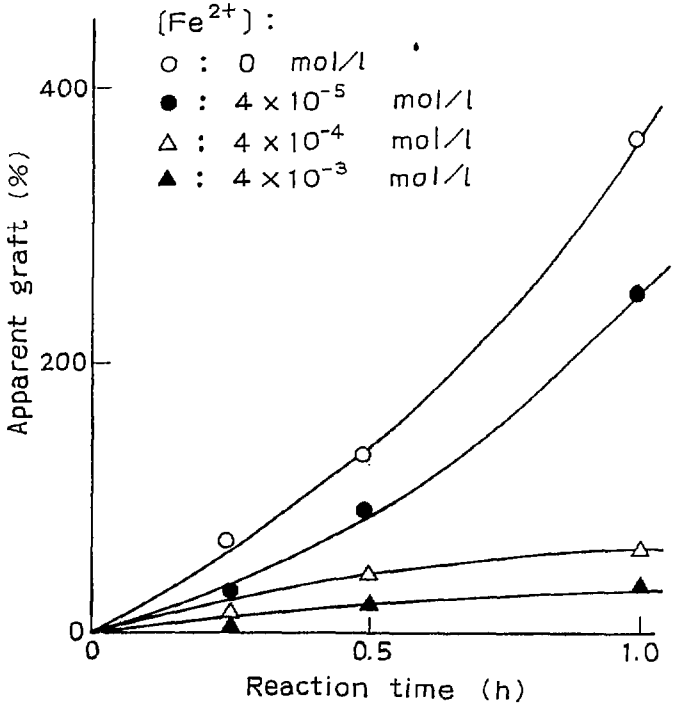

Fig. 6 Effect of the Mohr's salt on the grafting: pre-irradiation dose, 1 Mrad; reaction temperature, 40°C.

polyethylene[6]. Therefore, we assume that below 38°C the migration of radicals in the crystalline regions is the rate determining step and that for above 38°C, the reaction of monomers with radicals.

The degree of grafting is plotted as a function of reaction time at different concentration of Mohr's salt at 40°C in Fig. 6 and at 20°C in Fig. 7. The rate of grafting decreased with increasing concentration of Mohr's salt at both temperatures, indicating ferrous ion involves in the termination (1) of the propagating reaction.

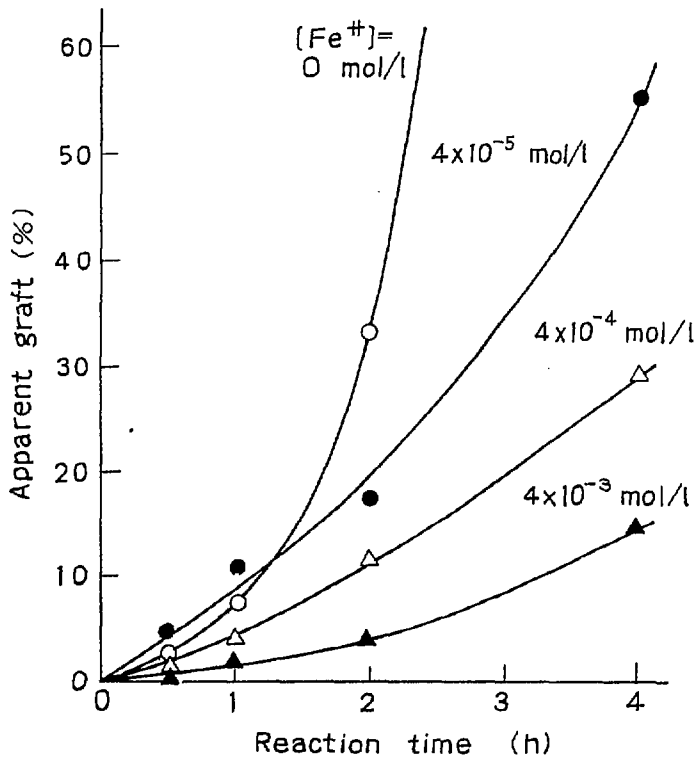

Fig. 7 Effect of Mohr's salt on the grafting:
pre-irradiation dose, 1 Mrad;
reaction temperature, 20°C.

$$\sim \dot{C}H_2 + H^+ + Fe^{2+} \rightarrow \sim CH_3 + Fe^{3+} \quad (1)$$

The rate of redox reaction (2),

$$ROOH + Fe^{2+} \rightarrow RO\cdot + OH^- + Fe^{3+} \quad (2)$$

seems not to be high enough to compete with the termination reaction (1) under the reaction conditions employed here.

Examination of the grafted surface by a scanning electron microscope revealed that the surface structure of the grafted layer strongly depends upon the presence of Mohr's salt. Further studies are in progress to obtain thin surface-grafted layer.

(K. Kaji)

1) T. Okada, K. Kaji, and I. Sakurada, JAERI Report 5027, 50 (1971).
2) K. Kaji, T. Okada, and I. Sakurada, Sen-i Gakkaishi, 33, T-12 (1977).
3) K. Kaji, T. Okada, and I. Sakurada, Radiat. Phys. Chem., 18, 503 (1981).
4) K. Kaji, J. Appl. Polym. Sci., 28, 3767 (1983).
5) G. H. Miller and E. W. R. Steacie, J. Amer. Chem. Soc., 80, 6486 (1958).
6) M. Takayanagi and T. Matsuo, J. Macromol. Sci. Phys., 1, 407 (1967).

III. LIST OF PUBLICATIONS

[1] Published Papers

1. K. Matsuda, T. Takagaki, Y. Nakase, and Y. Nakai, "Radiation Shielding and Dose Distribution of the High Dose Rate Electron Accelerator Room", JAERI-M 83-057 (1983).

2. K. Matsuda, Y. Nakase, Y. Tsuji, and I. Kuriyama, "Effect of Atmosphere on the Thermoluminescence of Irradiated Polyethylene", Rept. Prog. Polym. Phys. Japan, 27, 535(1984).

3. Y. Shimizu, S. Nagai, and M. Hatada, "Radiation Effects on Methane in the Presence of Molecular Sieves", J. Chem. Soc. Faraday Trans. 1, 79, 1973 (1983).

4. S. Nagai, "Current Aspect of Research on Desorption under Particle Bombardment", JAERI-M 83-235 (1983).

5. S. Sugimoto and M. Nishii, "Chemical Reactions of Carbon Monoxide and Hydrogen Induced by Electron Irradiation. III. The Reaction under Forced Circulation under Elevated Pressure", JAERI-M 83-126 (1983).

6. M. Hatada and S. Sugimoto, "Chemical Reaction of Methane/Ethane and Methane/Ethylene Mixtures by Electron Beam Irradiation", JAERI-M 83-229 (1983).

7. Y. Nakase and I. Kuriyama, "Wide-Angle X-ray Scattering of Poly(Tetraoxane) Obtained by Radiation-Induced Polymerization in the Solid State", Polymer J., 15, 231 (1983).

8. M. Nishii, K. Hayashi, I. Kuriyama, and S. Okamura, "Chemical Structure of Polyacetylene Prepared by γ-Ray in the Plastic Crystalline State", Rept. Prog. Polym. Phys. Japan, 26, 555 (1983).

9. J. Takezaki, K. Hayashi, and S. Okamura, "Molecular Weight Distribution of Polymer Latex by Radiation-Induced Emulsion Polymerization of Styrene", Reprt. Prog. Polym. Phys. Japan, 557 (1983).

10. K. Kaji, "Grafting of Poly(Acrylic ACid) onto Polyethylene Filament and Its Distribution", J. Appl. Polym. Sci., 28, 3767 (1983).

11. Y. Nakase and I. Kuriyama, "Modification of Polymer Material by Radiation", Genshiryoku Gakkaishi, 25, 529 (1983).

[2] Oral Presentations

1. K. Matsuda, Y. Nakase, I. Kumakiri, and Y. Tsuji, "Effect of Atmosphere on the Thermoluminescence of Irradiated Polyethylene", Annual Meeting of the Atomic Energy Research Society of Japan (Osaka), Apr. 4 , 1983.

2. S. Nagai and Y. Shimizu, "Studies on Desorption of Water from Silica Gel as studies by SIMS", The 36th Meeting of the 141st Committee of the Japan Society for Promotion of the Science (Osaka), May 19, 1983.

3. S. Nagai and Y. Shimizu, "The Water-Gas Shift Reaction Induced by Electron Beam Irradiation", The 7th International Conference on Radaition Research (Amsterdam), Jul. 7, 1983.

4. S. Nagai, "C-one Chemistry by Radiation--The radiation Chemical Reaction on Solid Surface", Symposium on Fundamental and Applied Radiation Chemistry at the Institute for Scientific and Industrial Research, Osaka University (Suita), Feb. 3, 1984.

5. S. Nagai and Y. Shimizu, "SIMS Study on Ion Imapct Desorption of Water from Silica Gel", The 4th International Conference on SIMS (Minoo), Nov. 19, 1983.

6. M. Hatada and S. Sugimoto, "Initial Products from Methane under Electron Irradiation", Annual Meeting of the Chemical Society of Japan (Sapporo), Aug. 28, 1983.

7. S. Sugimoto and M. Hatada, "Effect of Gamma-ray Irradiation on Methane under Elevated Pressures--Increase of the Yields of Higher Hydrocarbons by the Addition of a Small Amount of Ethylene", Annual Meeting of the Chemical Society of Japan (Sapporo), Aug. 30, 1983.

8. M. Hatada and K. Matsuda, "SIMS-Auger Study of Organic Layers on Gallium Arsenide", The 4th International Meeting on SIMS (Minoo), Nov. 16, 1983.

IV. EXTERNAL RELATIONS

The local meeting of the working group on "Plasma-Wall Interactions" met at the laboratory on June 16 when 10 scientists gathered to discuss the current aspects of their research.

A group of Chinese Government officials and scientists visited the laboratory on Nov. 9 to discuss about the current studies and utilization of irradiation facilities in the laboratory and to exchange our mutual interest on future radiation chemistry. The visitors were Mr. Le Fengming, Mr. Cai Dalie, Prof. Sun Jia Zheng, Mr. Zhon Shiliang, Mr. Gon Liansheng, Mr. Chen Jie, and Mr. Hsu Hui Kang.

Dr. N. White of Broken Hill Proprietary Co. of Australia visited on Mar. 6 to discuss the radiation effects on adsorbed molecles at the catalysis surface.

A training program for scientists and engineers in industries and government organizations was held in the laboratory. This one week program starting Oct. 19 included lectures and laboratory experiences concerned with the radiation chemistry of polymers.

Some studies in this laboratory were conducted under the cooperative agreements with Prof. Y. Tsuji of Kinki University and Prof. H. Saito of Osaka University. A joint research was carried out with the Dai-nichi Electric Cables Co. and a sponsored investigation was made under the contract with the Mitsubishi Electric Corporation.

V. LIST OF SCIENTISTS

(Mar . 31, 1984)

[1] Staff Members

Isamu KURIYAMA	Dr., polymer physicist, Director
Seizo OKAMURA	Professor emeritus, Kyoto University
Motoyoshi HATADA	Dr., physical chemist
Yoshiaki NAKASE	Dr., polymer chemist
Siro NAGAI	Dr., physical chemist
Shun'ichi SUGIMOTO	Physical chemist
Koji MATSUDA	Radiation physicist
Jun'ichi TAKEZAKI	Physical chemist
Masanobu NISHII	Dr., polymer chemist
Torao TAKAGAKI	Radiation physicist
Kanako KAJI	Dr., polymer chemist
Yuichi SHIMIZU	Physical chemist